

Assessing the impact of future greenhouse gas emissions from natural gas production

Daniel J G Crow*, Paul Balcombe, Nigel Brandon, Adam D Hawkes

*Sustainable Gas Institute,
Imperial College London,
London SW7 2AZ, UK*

Abstract

Greenhouse gases (GHGs) produced by the extraction of natural gas are an important contributor to lifecycle emissions and account for a significant fraction of anthropogenic methane emissions in the USA. The timing as well as the magnitude of these emissions matters, as the short term climate warming impact of methane is up to 120 times that of CO₂. This study uses estimates of CO₂ and methane emissions associated with different upstream operations to build a deterministic model of GHG emissions from conventional and unconventional gas fields as a function of time. By combining these emissions with a dynamic, techno-economic model of gas supply we assess their potential impact on the value of different types of project and identify stranded resources in various carbon price scenarios. We focus in particular on the effects of different emission metrics for methane, using the global warming potential (GWP) and the global temperature potential (GTP), with both fixed 20-year and 100-year CO₂-equivalent values and in a time-dependent way based on a target year for climate stabilisation. We report a strong time dependence of emissions over the lifecycle of a typical field, and find that bringing forward the stabilisation year dramatically increases the importance of the methane contribution to these emissions. Using a commercial database of the remaining reserves of individual projects, we use our model to quantify future emissions resulting from the extraction of current US non-associated reserves. A carbon price of at least 400 USD/tonneCO₂ is effective in reducing cumulative GHGs by 30 - 60 %, indicating that decarbonising the upstream component of the natural gas supply chain is achievable using carbon prices similar to those needed to decarbonise the energy system as a whole. Surprisingly, for large carbon prices, the choice of emission metric does not have a significant impact on cumulative emissions.

Keywords: methane emissions; upstream natural gas; global warming potential; emission metric; cost of carbon

*Corresponding author
Email address: dc08@ic.ac.uk (Daniel J G Crow)

1. Introduction

1.1. Background

Methane emissions make the second largest contribution to global greenhouse gas (GHG) radiative forcing, accounting for approximately 18% - not including indirect effects - compared to 64% from CO₂ [1]. Methane emissions originate from natural sources (e.g. wetlands, the oceans, termites), agriculture (e.g. cattle, rice fields), biogas, waste and the incomplete combustion of fossil fuels [2]. Approximately 10-15% of annual, global methane emissions arise from oil and gas supply chains and use [2].

With the increasing availability and production of natural gas globally [3], methane emissions are under growing scrutiny. Methane emissions have been shown to be highly variable across the gas supply chain, across regions, field environments, processes and equipment [4]. Additionally, their distribution is typically heavily skewed, suggesting that while most supply chains exhibit relatively low emissions, there is strong influence from a small number of higher emitters (so-called “super emitters”)[5]. There has been much progress on internalising the costs of CO₂ with carbon prices in key regions across the world (notably the EU’s *Emissions Trading Scheme* [6]), but although there has been a growing focus on the importance of methane emissions, there are currently few internalisations of their cost¹.

Methane is a very strong but relatively short-lived GHG compared to CO₂. It has approximately 120 times greater radiative forcing than CO₂, but an average perturbation life of only 12.4 years, so its climatic impact decays rapidly. In comparison, CO₂ has a complex atmospheric lifetime: 50% is removed after 37 years, but 22% effectively remains in the atmosphere indefinitely. The Global Warming Potential (GWP) is typically used to compare the climate impacts of different GHGs relative to CO₂ over an average time period of 100 years. However, different time horizons affect the assumed impact of methane and increasingly a wider range of time horizons and metrics are being used [8]. Key alternatives to GWP are the use of global temperature change potential (GTP) and dynamic metrics which follow the impacts over time rather than using a single time horizon based on a fixed number of years after the emissions take place.

In a political environment in which limiting radiative forcing becomes ever more critical, a market-based mechanism for limiting methane emissions becomes an option [9]. This may be as part of a carbon price [7], or perhaps preferably as a separate methane price. The impact of a methane price on gas well development may be significant given the variability in methane emissions described above. Depending on the cost and timing of future emissions, undeveloped, or even currently producing natural gas fields could turn into “stranded assets”

¹The *Californian Air Resource Board’s* Cap-and-Trade scheme is unusual in including methane as a CO₂ equivalent [7].

1.2. Existing approaches

Methane emissions as externalities. While much effort has been put to representing the cost and environmental impacts of natural gas production and infrastructure development, there has been little focus on internalising methane emissions to our knowledge. Some recent studies have investigated the impacts of a methane price or tax on agricultural practices, for cattle rearing [10] [11], and different methods of regulating or reducing methane emissions from the gas sector are assessed in [9] from a policy perspective, where it is suggested that a direct tax on emissions may be preferable to technological or performance-based standards in terms of cost and environmental effectiveness. However, no studies were found that estimate the cost impact of a methane tax on the oil and gas industry.

The timing of emissions and climate impact. There has been little attention paid to accounting for the timing of emissions and its climate impact, although Edwards and Trancik [12] suggest that timing plays a key role in determining the climate impact. Using different GWPs with an explicit time horizon, Levasseur et al. focussed on the climate impact over time of different transport fuel options via dynamic assessments to demonstrate the importance of emissions timing [13]. A similar study by Roy et al. [14] on dynamic emissions impacts used an optimisation model to determine the portfolio of transport technologies which maximise energy consumption while meeting a radiative forcing stabilisation target. More generally, the difficulties of using static GWPs has also received some attention, both for models of climate forcing [15] and integrated assessment models (IAMs) [16], where the choice of GWP can impact GHG abatement and cost.

In studies of oil and gas, one empirical model [17] of CO₂ emissions from Norwegian oil and gas fields found that emissions intensity is negatively correlated with production, suggesting a temporal trend towards higher emissions intensities at the end of a field's lifecycle. Similar findings were reported by Brandt [18] in a case study of the energy efficiency of oil production in hundreds of Californian oil fields. One recent more detailed study [19] used data from 25 giant oil fields worldwide to construct a probabilistic model of GHG emissions arising from oil production as a function of time. Although multiple GHGs are taken into consideration, results are quoted in terms of total GHGs emitted, with no information about the CO₂/methane breakdown. Statistical analysis on field measurements of methane leaks [20] has also found correlations with well age and production rates, but low R^2 -coefficients (< 0.1) suggest that the main drivers of emissions from individual sites are stochastic variables related to maintenance and/or the specifics of production rather than the production rate *per se*. Focusing exclusively on the production of unconventional gas from the Marcellus shale basin, a GHG life cycle analysis was done by Jiang et al. [21] which includes estimates of CO₂ and methane emissions by activity type (site preparations, drilling etc.) from which some temporal trends can be inferred. However, to our knowledge, estimates of the climate impact of GHG emissions from natural

gas production have not thus far used dynamic climate metrics, nor investigated the potential cost impacts if those emissions were to be internalised.

1.3. Aims of this study

This study has three main aims. First, to estimate the time dependence of GHG emissions in the US upstream gas industry, both on the level of individual fields and nationally, in terms of the future production of reserves in existing fields. Second, to examine the interplay of the timing of emissions with the choice and implementation of an emission metric, especially in cases when the emission metric is also time-dependent. Third, to elicit the impact of future carbon pricing scenarios on the profitability and volume of current US reserves, using a range of different emission metrics.

This study is novel on a number of fronts. It is the first which attempts to internalise the cost of methane emissions from natural gas supply by combining deterministic models of emissions and the economics of production for a single field. This is also the first study to account for both the timing of emissions across a national population of natural gas fields, and the impact of the timing of emissions on the climate via the use of dynamic climate metrics.

The rest of this paper is organised as follows. First, Section 2.1 describes the techno-economic approach to gas field modelling in the DYNAAMO model. Estimates of GHG emissions are presented in 2.2, including a discussion of climate potentials, the impact of methane and the costs of emissions from different stages of production, and carbon pricing. Results are displayed in Section 3; first for the emissions profiles of individual representative fields (Section 3.1), and then for aggregated emissions from current US reserves (Section 3.4). Last, Section 4 summarises the main findings of this paper, compares these to those in other reports and briefly discusses their policy implications.

2. Methodology

Energy systems modelling. Energy systems models [22] [23] and integrated assessment models² [24] have been developed to study long-term transitions of the energy system. Though they vary widely in geographical and temporal scope, resolution, and modelling approach, most are techno-economic models which incorporate policy and environmental dimensions to help inform decision-making about investments in energy assets, technological R&D, and the potential impacts of future climate change mitigation policies. The likely role of fossil fuels - and particularly natural gas - in the global energy system in the near term [25] [3] makes it essential to understand how and when emissions associated with their production will occur. In “well-to-wheel” assessments of climate impact, most IAMs handle

²Integrated assessment models are similar to energy systems models in terms of scope and purpose, but often incorporate environmental feedbacks as well as emissions from non-energy sources, such as land use.

emissions from the oil and gas sector relatively crudely, often using representative GHG intensities for extraction, processing/refining and transportation to market. CO₂ emitted during extraction is normally attributed to “own-fuel” burn, which can be $\sim 5 - 10\%$ of production by volume [26] [27] [28]. One limitation to modelling the temporal aspect of upstream emissions has been the relatively simplistic treatment of gas production. Most modelling efforts focus on the international gas trade [29] [30], using static representations of the availability of resources at a given cost [31] [32]. Dedicated models of emissions from (especially unconventional) natural gas production exist [21] [33] [34] [35], but often lack information about when the emissions occur, their nature (CO₂/methane), and their impact on the economics of supply (breakeven prices, cashflows etc.).

2.1. The DYNAAMO model

DYNAAMO is a recently developed model of natural gas supply which builds dynamic supply curves by aggregating incremental production on a sub-field level. Decades long data series [36] [37] from thousands of gas fields worldwide are used to establish a realistic picture of both production and expenditure patterns over the lifecycle of a typical field. This enables DYNAAMO to calculate breakeven prices which reflect not only the operating environment (Shale plays, Deepwater etc.) but also the size and age of the field. Such detailed representation of the *timing* of cashflows makes DYNAAMO a useful tool for the present study, where - both in terms of their changing environmental impact with respect to a future stabilisation horizon and a rising carbon price - the timing of future emissions is key in determining their impact on the economics of upstream gas. A comprehensive description of DYNAAMO can be found in [38]; Appendix B provides an overview of those features of the model most important for this work.

Although the results of this study should be relevant to the upstream industry globally, the focus is here restricted to the USA for two main reasons. First, there is a wealth of historic data - both techno-economic and emissions related - which can be used to calibrate the model (detailed emissions estimates for other regions are hard to find). Second, production in the US is historically the most diverse of any region with significant natural gas resources, providing an interesting comparison of the impact of emissions in different field environments. The field environment is a combination of technology and operating environment with distinctive production and cost characteristics. Five major field environments account for almost all natural gas production in the USA, as set out in Table 1. For each field environment DYNAAMO constructs a prototypical field lifecycle profile based on the³ 2P

³The term 2P stands for the sum of the proven and probable reserve estimates. A reserve is classified as proven if it is likely that 90% or more of that resource can be profitably recovered in the current economic climate. Probable reserves are deficient in geological data, making their presence and profitability uncertain. To compensate for this, the gross estimate is reduced by 50%.

Field Environment	Description	2P Remaining Reserves (BCM)
Shelf	Offshore fields in a water depth <400m	37.95
Deepwater	Offshore fields in a water depth >400m	8.06
Onshore Conventional	Onshore, mainly sandstone reservoirs which achieve commercial production rates without hydraulic fracturing	366.77
Tight/Shale	Onshore sandstone and shale reservoirs which require horizontal wells with hydraulic fracturing	13139.02
Coal bed methane	Onshore natural gas extracted from coal seams	114.33

Table 1: Remaining 2P reserves of natural gas in US fields containing dry gas or a mixture of dry gas and condensates in 2018 [37]. “Associated” gas reserves in fields developed to produce oil are excluded from this study. The 5 field environments considered account for > 97% of US domestic production from reserves in non-associated fields.

estimated ultimate recovery (EUR) of the field. All aspects of the expenditure and production profile modelling are informed by historic data for US fields [36] [37]. The field lifecycle profile specifies expected cashflows as a function of time and so can be used to compute the net present value (NPV) of each field as a function of its age and the hub price for natural gas. The lowest price for which the NPV is positive defines the “breakeven” price for a particular field (see Appendix B). Emissions costs are assumed to be paid concurrently with emissions⁴. The main effect of emissions costs in DYNAAMO is to reduce cashflows and the NPV of a field, but raise its breakeven price, which in turn reduces its EUR, as cost-marginal resources become uneconomic to extract.

2.2. Emissions

2.2.1. Estimating CO₂ and methane emissions in the US upstream gas industry

Table 2 shows estimates of CO₂ and methane emissions respectively. All values were taken from the review of Balcombe et al. [4], which analysed 250 studies on methane and CO₂ emissions associated with different stages of the natural gas supply chain. There have been numerous other publications on the topic of methane emissions from US natural gas supply chains since this study, including notably [39] [40] [41]. Broadly, the range of estimates of emissions from these more recent studies bound those reported here, which have a sufficient level of disaggregation to enable the modelling undertaken in the

⁴When companies report emissions figures for the previous year it is envisaged that a carbon tax would be levied on these as part of overall fiscal expenditure (“government take”).

present study. The values in Table 2 were transformed from g/MJ of delivered gas on a higher heating value basis to g/Sm³ produced at the well head. A higher heating value of 38.1 MJ/m³ was used and it was assumed that the total gas loss from production to delivery was 11.5% [4]. The range of emissions represents the minimum, median and 95th percentile estimate from the literature reviewed. This includes many types of regions, technologies and operations, as described in [42]. We believe that this represents the broad range of supply chain emissions seen across regions and technologies. The maximum values were not included as they are often one or two orders of magnitude greater than the median values and so the 95th percentile is used to illustrate the relatively constrained range within which the vast majority of estimates lie. From subsequent analysis of the data sources [5], it is clear that the use of emissions minimising technologies such as *reduced emissions completions* (RECs), vapour recovery units and liquids unloading plunger lifts represent the lower limits of emissions, but technology selection does not account for all the variation and so we are not prescriptive of the technology across this range: operational and maintenance strategies are key in constraining emissions and minimising the potential for a “heavy-tailed” distribution. Emissions intensities for onshore conventional and unconventional are differentiated given the available data [43, 44, 45, 46, 47, 48, 49, 50, 51]. However, no such data were found for offshore facilities, and so these were assumed to be similar to onshore conventional. Note that offshore emissions may be less than those quoted in Table 2 given the more stringent safety requirements which apply offshore, but there is little in the way of transparent data to support this.

While the range of emissions included here is large and encompasses a broad range of supply chains and technical and operational configurations, the GHG emissions profiles of gas production are assumed to remain the same irrespective of e.g. a future carbon price. In reality it is likely that with increasing pressure on climate impacts, emissions per unit of produced gas will fall. Best practices will improve over time driven by efficiency improvement and regulation. For example, the improvement of cost-effective methane emissions monitoring and detection (e.g. via [52]) may deliver substantial further reductions in fugitive emissions. The projection of emissions reductions is outside of the scope of this study, but the impact of lowering emissions intensity would be to reduce the risk of asset stranding.

2.2.2. Assessing the impact of methane

The global warming potential (GWP) is normally used to compare the relative impact of different GHGs by converting emissions into CO₂ equivalents. It is defined as the average (time-integrated) radiative forcing of a pulse emission over a defined time horizon, compared to the equivalent forcing from CO₂. Typically a 100 year time horizon is used, giving CO₂ equivalent multiples in the range 28 - 36 for methane (depending on whether indirect climate impacts are included) [53]. However, there are increasingly calls for the use of either different time horizons or different metrics altogether [54] [8]

Stage	Sub-stage	Methane (g/Sm ³)			CO ₂ (g/Sm ³)		
		Low	Central	High	Low	Central	High
Pre-production	Site preparation	-	-	-	0.3	5.8	22.7
	Drilling	-	-	-	0.3	7.3	22.2
	Hydraulic fracturing	-	-	-	4.6	7.3	20.2
	Completion (Uncon.)	-	0.03	0.24	-	0.5	4.3
	Completion (Con.)	-	0.04	0.06	-	0.7	1.1
Extraction	Onshore (Uncon.)	1.08	3.20	9.37	4.8	14.3	55.5
	Onshore (Con.)	1.08	3.22	8.26	4.8	14.6	35.1
	Deepwater	1.08	3.22	8.26	4.8	14.6	35.1
	Shelf	1.08	3.22	8.26	4.8	14.6	35.1

Table 2: Estimates of upstream methane and CO₂ emissions intensities for natural gas fields in the USA in grams per standard cubic metre of gas extracted.

because of: the dependency of the metric on the selected time horizon; the fact it does not compare gases against their impact on global temperature; and that it measures an average climate forcing effect of a single pulse emission over time but gives no indication of the climate impact at an end-point in time, or that of a sustained emission. The global temperature change potential (GTP) addresses some of these concerns as it compares gases in terms of their impact on temperature change and it estimates the impact at an end-point rather than as an average impact over time [55]. It is defined as the change in mean surface temperature after a specified time due to a pulse emission, relative to the effect from an equivalent pulse emission of CO₂. Consequently it also requires the selection of a time horizon, which has a large impact on the equivalency value for methane, as shown in Fig. 1.

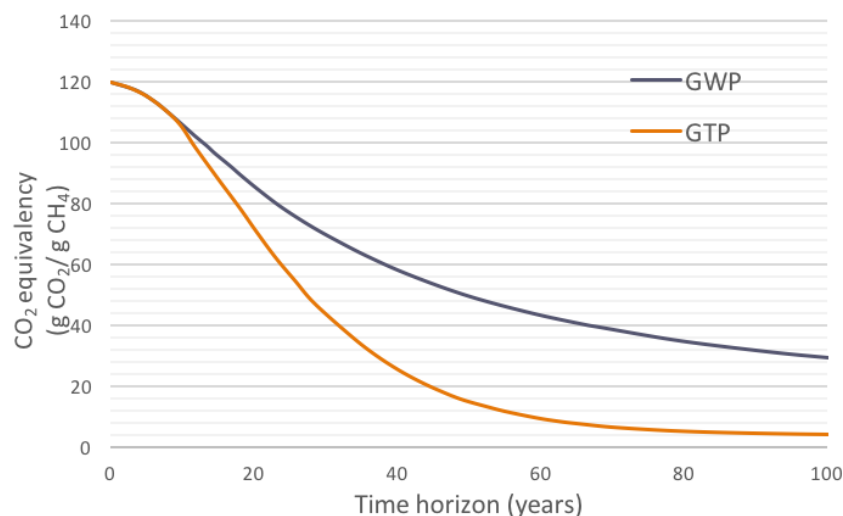


Figure 1: CO₂ equivalency values across different time horizons for the Global Warming Potential and the Global Temperature Change Potential. Source: [56].

Given the complexity of the impact of methane and carbon dioxide in the atmosphere, the application of dynamic climate metrics has been suggested as a compromise between simple static metrics such as GWP/GTP and full climate models, which are often infeasible to incorporate into regional or small scale technology studies [13] [54]. Dynamic metrics differ from static metrics in that they are internally consistent in specifying an end-point, rather than a moving time-horizon depending on when emissions occur. Static metrics used to estimate emissions of a natural gas well, for example, implicitly treat those emissions as originating in a single pulse, whereas the well in question may be active and emitting sporadically for 25 years or more. If a well emits within the first year of operation, say 2015, the GWP100 would consider the impact up to 2115. If the well still operates and emits in 2045, the GWP100 estimation would consider the impact up to 2145. The use of static metrics in this way has two drawbacks: from a climate perspective it is hard to fix a “stabilisation year” and associated budget of cumulative emissions, and from a techno-economic perspective it is hard to compare facilities which emit at different rates over different time periods. However, both GWP and GTP can be used “dynamically”, where the end-point is fixed and in a multi-year emissions assessment, as the year of emission increases, the time period decreases. The result is that any methane emissions incurred at the start of the time frame contributes relatively little, but the values can increase significantly as the emissions approach the end-point. In order to employ a dynamic metric, a time horizon must be selected (e.g. 2100), which may be in accordance with a presumed climate stabilisation year. For an emissions assessment, the emissions in each year will be multiplied by a different CO₂ equivalency (e.g. emissions in 2020 are multiplied by GWP80, those in 2021 by GWP79 and so on).

2.2.3. Modelling the costs of emissions

Variable Emissions. Variable emissions are directly related to the extraction of gas from the field. Both methane and carbon dioxide emissions are produced at varying degrees from pre-production, extraction, processing as well as downstream. Carbon dioxide emissions chiefly arise from the combustion of fuel used during operation, from flared gas or from venting of the waste CO₂ content in raw gas. Methane emissions occur via operational and intermittent vents, incomplete combustion of gas and fugitive emissions, which may be from any fluid-contacting equipment. Key contributors to methane emissions include leaks from compressor (or other) seals, from the use of gas-driven pneumatic valves, liquid storage tank vents and liquids unloading. For a detailed account of the mechanisms and equipment associated with these emissions, see [4].

Variable emissions are dominated by methane leaks and are paid per volume of gas extracted through the carbon price, cpr_t (in MUSD/tonneCO₂), and the variable emissions intensity, $VE_{t,n,i}$ (both of which can change with time). The variable emissions intensity has units of tCO₂e/BCM and is given by,

$$VE_{t,n,i} = VCO_2^i + P_{t,n} \cdot VCH_4^i \quad (2.1)$$

where VCO_2^i and VCH_4^i are variable (i.e. gas extraction-related) CO₂ and methane intensity of gas produced respectively (corresponding to the figures in the “Extraction” stage of Table 2) and $P_{t,n}$ is a (in general time varying) conversion factor (such as GWP or GTP) which converts methane emissions into their CO₂ equivalent. As before, t denotes the year, n the age of the field and i the asset class or field environment. The variable emissions profile of a field is thus given by multiplying the production profile in Eq.(B.1) by VCO_2^i or VCH_4^i for CO₂ and methane respectively.

Fixed Emissions. In contrast to variable emissions, fixed emissions are dominated by CO₂ and occur at every stage of operations, independently of production. The fixed emissions intensity has units of tCO₂e and is given by,

$$FE_{t,n,i} = FCO_2^{n,i} + P_{t,n} \cdot FCH_4^{n,i} \quad (2.2)$$

where $FCH_4^{n,i}$ and $FCH_4^{n,i}$ are fixed CO₂ and methane emissions in month n of the project lifecycle respectively and $P_{t,n}$ is the CO₂ equivalent of methane as in Eq.(2.1). Fixed emissions have two contributions: from site preparations and from drilling activities (including the “hydraulic fracturing” and “well completions” sub-stages in Table 2). Emissions from site preparations can be modelled simply by spreading them uniformly over the pre-production phase of operations. In contrast, drilling activities depend on both the age of the field and the field environment, and so drill-related emissions need to be treated more carefully.

2.2.4. Emissions associated with drilling activity

The time variation of emissions associated with drilling activities is governed by the *drilling profile* of the field. The drilling profile describes how drilling activity - drilling, hydraulic fracturing and well completions - changes over the lifecycle of the field.

Conventional vs. unconventional fields. There are major differences in the timing and nature of drilling activities for conventional and unconventional fields. For conventional fields, fewer wells are drilled, hydraulic fracturing is absent and most activity occurs during the pre-production and ramp-up phase of a project. Typically, a small number of “appraisal” wells are spudded early in project cycles prior to or during the pre-production phase to ascertain the volume of hydrocarbons and reservoir pressure⁵ [57]. These are followed by “development” wells which are drilled to extract gas for commercial purposes. The number of development wells depends on a combination of factors including the wellbore diameter, the reservoir porosity, the wellhead pressure and the desired plateau rate of production for the field. As a guide, 306 appraisal and 918 development wells were drilled in the South North Sea basin (i.e. conventionals) between 1980-2010, with an average of 1.7 appraisal and 5.1 development wells per field [58]. The majority of development wells were spudded and completed within an 18 month period at the start of the ramp-up phase, with their subsequent (time-averaged) production showing no significant decline for a period of between 5-15 years after completion [59] [60]. Drilling activity is also common later in the lifecycle of conventional fields in order to maintain production rates as pressure in the central reservoir drops off. This can be “infill” drilling, which is the addition of wells within a proven reservoir to boost the speed and volume of ultimate recovery and/or “step-out” drilling which is used to look for reservoir extensions surrounding the developed reservoir which can be tied-back to the main platform [57]. Such infrastructure-led drilling activities occur towards the end of the plateau phase and typically comprise 10 – 20% of the total drilling activities of a project [61]. Based on this analysis, this study assumes that for conventional fields emissions associated with drilling activity are spread between the ramp-up phase and late-plateau phase in a 4 : 1 ratio. Adding the emissions due to site preparations, $CO_{2,prep}$, gives the following for the fixed part of the CO_2 emissions profile for

⁵So-called “wildcat” wells may be drilled as part of the exploration process, often many years before site preparations begin. Because of the high variability in the timing of these wells and their small number compared to development wells, emissions associated with drilling of wildcats is neglected in this study.

conventional fields:

$$\text{FCO}_2^{n,i} = \begin{cases} \frac{1}{N_r} \cdot R_{0,i} \cdot \text{CO}_{2,\text{prep}} & -N_r \leq n < 0 \\ \frac{1}{N_p - N_r} \cdot 0.8 \cdot R_{0,i} \cdot \text{CO}_{2,\text{drill}} & N_r \leq n < N_p \\ 0.1 \cdot R_{0,i} \cdot \text{CO}_{2,\text{drill}} & N_d - 1 \leq n \leq N_d \\ 0 & \text{otherwise} \end{cases} \quad (2.3)$$

This emissions profile (Eq. 2.3) treats emissions from site preparations as spread equally over the period before a field goes on-stream, and those resulting from drilling activities as spread equally over the ramp-up phase and the last two years of the plateau phase of production.

For unconventional fields, the exploratory and appraisal phases are similar to those of conventional fields, but the timing of drilling activities associated with production is radically different. Individual wells incur high initial decline rates and additional wells must be drilled and fractured on an ongoing basis to ensure that production is maintained at commercially viable rates⁶. At any given time, the total production from a field results from aggregating the production of many wells drilled at earlier stages in the field lifecycle. This means that the production profile can be used to estimate the drilling profile. For this study we use well level data to build a simple model of drilling activity over the lifecycle of typical conventional and unconventional fields, and from this derive estimates of the associated fixed emissions as a function of time (see Appendix A for details). This approach results in the following emissions profile for unconventional fields,

$$\text{FCO}_2^{n,i} = \begin{cases} \frac{1}{N_r} \cdot R_{0,i} \cdot \text{CO}_{2,\text{prep}} & -N_r \leq n < 0 \\ \bar{\lambda}(n) \cdot R_{0,i} \cdot \text{CO}_{2,\text{drill}} & 0 \leq n < N \end{cases} \quad (2.4)$$

where $R_{0,i} \cdot \text{CO}_{2,\text{prep}}$ are the total CO_2 emissions from site preparations, spread over the N_r years of the pre-production phase, and $R_{0,i} \cdot \text{CO}_{2,\text{drill}}$ is the total contribution from drilling activities which is weighted by the drilling intensity $\bar{\lambda}(n)$ over the production phase of the field. The drilling intensity (derived in Appendix A) is a number between zero and one which describes the fraction of total drilling activity taking place in a given month of the field lifecycle. The fixed part of methane emissions, $\text{FCH}_4^{n,i}$, take the same form as Eq.(2.3) and Eq.(2.4), although these emissions are estimated as only a few percent of those associated with extraction and there is no contribution during site preparations (see Table 2). Combining variable and fixed emissions, the total mass of CO_2 produced by a field with

⁶The original wells may be refractured after a period to boost recovery, but (unlike the conventional case) this will normally be soon (12-18 months) after the start of production and the emissions involved can be taken as part of those associated with production.

EUR $R_{0,i}$ over its lifecycle is given by,

$$\text{total CO}_2 \text{ emissions} = R_{0,i} \cdot \text{VCO}_2^i + \sum_n \text{FCO}_2^{n,i} \quad (2.5)$$

where the sum is over all years up to and including decommissioning. An expression of the same form as Eq.(2.5) holds for methane.

3. Results

3.1. Estimating emissions profiles

To illustrate the results of the emissions profile modelling described in Section 2.2, estimates of these profiles for representative conventional and unconventional fields are shown in Fig. 2. The central estimate of methane emissions is similar for both field environments as the majority of these emissions are associated with gas extraction. However, the “high” estimate (shown as the upper bound of the error bars in Fig. 2) is substantially larger ($\approx +200\%$) for the unconventional field compared to the conventional field ($\approx +125\%$). The lower methane emissions during plateau in Fig. 2 (left) compared to Fig. 2 (right) is mainly a consequence of the smaller EUR of the unconventional field, as well as the lower emissions associated with completions (assuming the use of RECs [62]). Note that the high emissions values for unconvensionals represent non-RECs, but the central figures include RECs, which are on average lower than conventional completions (which do not need to use RECs). The total direct methane emissions from all upstream operations are 71.73 kt and 58.14 kt for the conventional and unconventional fields shown, corresponding to a slip rate of 0.47% and 0.46% of total extractions respectively.

CO₂ is emitted during site preparations, drilling activities and extraction. Conventional and unconventional field are drilled differently, resulting in a early-stage spike in emissions for conventionals followed by very low activity during the plateau phase. A possible further spike in CO₂ from late-stage “in-fill” or “step-out” drilling is shown in Fig. 2 (left).

3.2. GWP vs GTP

The estimated environmental and economic impacts of applying different climate metrics to the reference field emissions profiles (Fig. 2) are shown in Figs. 3 and 4. With static metrics, total GHG emissions peak early, especially for the conventional field (Fig. 3). The main effect of dynamic GWP or GTP equivalencies is to shift the emissions peak back towards the end of a field’s lifecycle, with the potential to increase enormously a company’s exposure to a rising carbon price. Bringing forward the stabilisation year heightens this effect, especially if the GTP metric is used. For the unconventional field, using a stabilisation year of 2100, peak emissions of 50 kt CO₂e (CO₂ equivalent) occur in

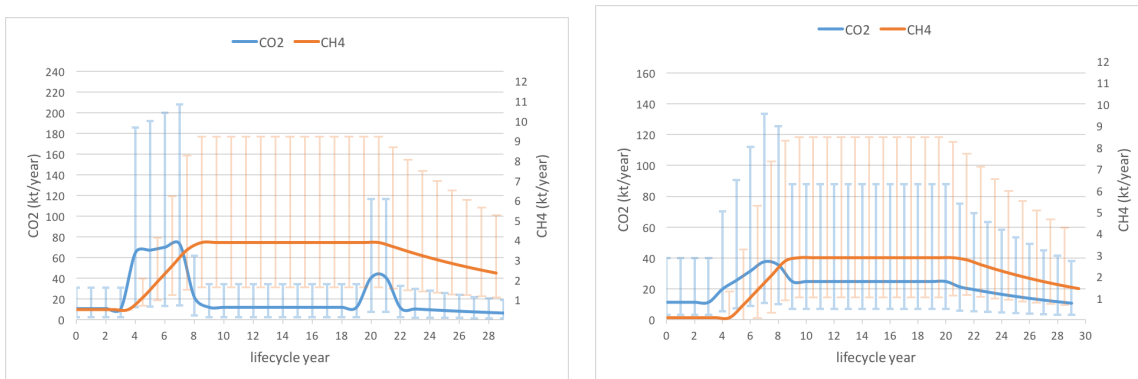


Figure 2: Emissions of CO₂ and methane (CH₄) over the lifecycle of a typical 22 BCM conventional field (left) and a 18 BCM unconventional field (right). The solid lines show central estimates and the bars represent the range of emissions intensities bounded by the “low” and “high” scenarios in Table 2 and described in Section 2.2.1. For the conventional field, production begins after 40 months, and the field goes on plateau in year 9. After year 21 production declines at a rate of 7.7% per year, with decommissioning in year 30. For the unconventional field, production begins after 40 months, and the field goes on plateau in year 9. After year 20 production declines at a rate of 8.6% per year, with decommissioning in year 29.

2023 (Fig. 4 (left)), with lifecycle emissions of 1061.1 kt CO₂e . Changing the stabilisation year to 2065 results in an emissions peak of 148 kt CO₂e in 2036 (Fig. 4 (right)) and lifecycle emissions of 2869.0 kt CO₂e. The sensitivity to stabilisation year can be understood by considering the typical length of project lifecycles (~ 30 years) and Fig. 1. Fields starting in 2015 will be coming off plateau between 2035-2040, and still extracting gas until around 2045. Methane emissions during this late phase of production are coupled to forcing potentials in the range GTP30 - GTP20 where the GTP equivalency curve is changing most rapidly. The static metrics GTP50 and GWP50 (i.e. corresponding to a stabilisation year of 2065 for a field starting in 2015) are shown for comparison.

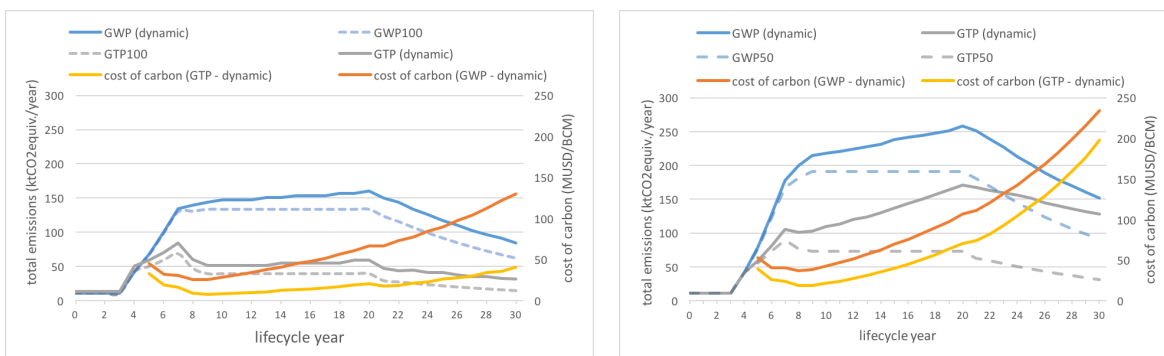


Figure 3: Total GHG lifecycle emissions profile for a conventional 22 BCM field (described in Fig.2 (left)) using both dynamic and static GHG potentials with a stabilisation year of 2100 (left) and 2065 (right). The lifecycle is assumed to begin in 2015, and emissions are based on the central estimates in Table 2. Also shown is the cost of these emissions per BCM of gas produced using the “conventional” carbon price scenario described in Appendix C.

To give a sense of the potential economic impact of these GHG emissions on the level of a single field, the cost of carbon per volume of gas produced is shown in Figs. 3 and 4. The cost of carbon is equal to the carbon price multiplied by the CO₂-equivalent emissions produced when lifting a BCM of gas, and takes the form of a variable opex or levy on production. This cost is based on pricing emissions using the “conventional” carbon price scenario (see Appendix C), which crosses 555 USD/tonne CO₂ in 2040, and using the production profiles described in Section 2.1. Despite a rising carbon price the cost of carbon initially decreases, especially for conventional fields, after drilling is completed, reaching a minimum a few years after production plateaus out (see Fig. 3). It rises most quickly during the decline phase due to the steepening carbon price, the fall-off in production and the increased forcing potential of the methane component. Note that the cost of carbon indicates an upper bound to the breakeven gas price which would shut down further production (as a guide, 3 USD/MMbtu \sim 105 MUSD/BCM).

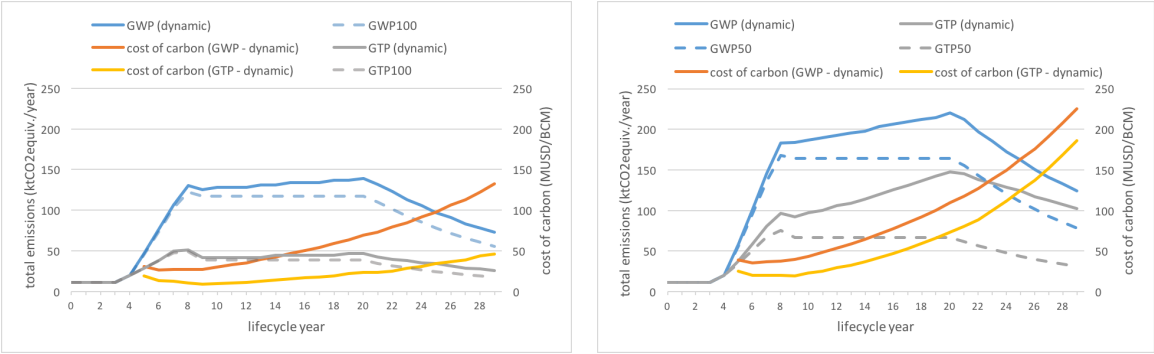


Figure 4: Total GHG lifecycle emissions profile for a unconventional 19 BCM field (described in Fig.2 (right)) using both dynamic and static GHG potentials with a stabilisation year of 2100 (left) and 2065 (right). The lifecycle is assumed to begin in 2015, and emissions are based on the central estimates in Table 2. Also shown is the cost of these emissions per BCM of gas produced using the “conventional” carbon price scenario described in Appendix C.

3.3. Changing the carbon price

This section focuses on how the carbon price could affect the initial NPV of an assortment of upstream projects and “strand” gas reserves. The carbon price is set by its annual growth rate (see Appendix C), with results presented for average carbon prices during the period 2015-2050, corresponding to a range of growth rates between 1 - 7%. For a given carbon price, we consider 35 hypothetical - yet representative - projects of different initial EURs taken from the distributions in Fig. B.12, with each project assumed to be at the start of its pre-production phase. Emissions of CO₂ and methane are internalised with the carbon price, using a GWP100 for methane for this case study. The initial

NPV is the sum of future cashflows, discounted at 10%⁷. Under a changing carbon price DYNAAMO calculates the economic limit of production and adjusts the production profile to maximize the forward NPV. It is the initial NPV corresponding to this optimized profile which is reported in Fig. 5 (right). The calculation of initial NPV is made using a fixed reference gas price, here taken as 3.5 USD/MMbtu (corresponding to the well head average from 2010 - 2015). In reality, it is likely that large carbon prices would have an effect on the demand for gas as well as the gas price. In the same vein, large carbon prices would likely force producers both to drive down costs and curtail emissions as much as possible by, for example, making large changes to drilling and production profiles. However, the purpose of the analysis here is neither to forecast market dynamics nor to anticipate the strategic behaviour of producers, but rather to examine the change in the *current* value and volume of reserves (which do not directly depend on gas demand) by field environment in different carbon prices scenarios.

On a single field level, “stranded” resources are those which are uncommercial due to the costs of emissions associated with their extraction. This can happen due to the modified production profile described above, but also because less profitable fields (normally smaller onshore fields) become inviable to develop from the outset. Fig. 5 (left) shows the percentage of EUR stranded at different carbon prices for representative individual fields. As the carbon price is raised initially, a cluster of predominantly CBM, Tight/Shale and Onshore conventional projects experience some stranding of reserves, while offshore fields are largely immune to modest emissions pricing. At around 200 USD/tonneCO₂ a single Tight/Shale project becomes unprofitable to develop and all reserves held in this field are therefore stranded. Some other projects become 100 % stranded as the carbon price is raised further, and beyond 910 USD/tonneCO₂ all the projects in the sample are expected to experience partial or total stranding of their gas reserves. Resources in Tight/Shale projects are especially vulnerable to stranding as their value suffers most as the carbon price rises. In contrast, CBM fields tend to be more resilient to the carbon price, due to their larger size (although the largest individual fields in the US are Tight/Shale, the average field size of CBM is around 6 times greater than Tight/Shale) and the fact that they are generally much shallower and therefore cheaper to drill than Tight/Shale [37] [64].

Fig 5 shows a difference between onshore and offshore fields in terms of stranding and value of resources. This reflects shorter average production cycles and the higher hurdle rates applied offshore. The longest production cycle in the suite of offshore fields reported here is 19 years: a hypothetical 500 BCM deepwater field with a 28 year production cycle would be expected to show large stranded

⁷A discount rate of 10% is consistent with that used in reference scenarios by other models [36] [63]. In a climate of high uncertainty about future emissions costs, companies could apply higher discount rates to reflect additional risks associated with longer payback times etc. . In this study the discount rate is held fixed to facilitate comparison of the effects of changing other variables (such as the emission metric).

volumes with commensurate losses to its initial value under the carbon price scenarios presented here.

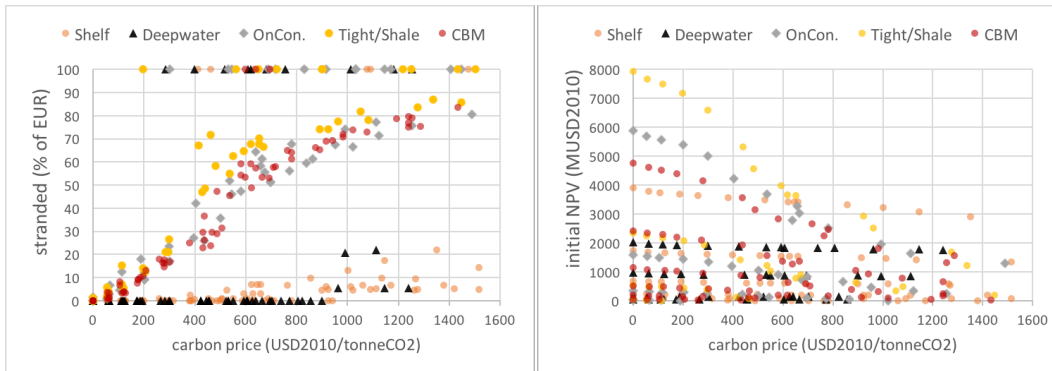


Figure 5: (Left) “Stranded” reserves for 35 representative projects, expressed as a percentage of 2P initial EUR, plotted against the average carbon price over the period 2015 - 2050. The emissions intensities are taken from central estimates in Table 2, and the carbon price rises exponentially with a ramp rate of between 1 – 7% per year. (Right) Initial NPV as a function of carbon price for the same 35 representative projects. Only projects with positive initial NPV are shown.

For small rises in the carbon price the response of average initial NPV is approximately linear. For every dollar increase in the average carbon price between 2015-2050, the value of reserves in the largest Tight/Shale fields lose around 0.03 MUSD per BCM, those in CBM fields around 0.04 MUSD per BCM and those in onshore conventional fields around 0.02 MUSD per BCM. Fig 5 (right), shows that large fields lose value most quickly due to their increased exposure to higher carbon prices. Small and medium size high value project types (with initial NPV-per-volume > 30 MUSD/BCM) are the most resilient to high carbon prices and are associated particularly with Deepwater and CBM field environments.

3.4. Future emissions from US gas fields

Having estimated the full-cycle emissions (and consequent economics) of individual representative gas fields, the focus of this section is on future emissions resulting from the production of current US reserves. Future natural gas production over the time frame considered here will involve both current 2P reserves as well as reserve additions and as-yet undiscovered resources in new fields and/or basins. 2P reserves are a techno-economic and not merely technical resource category: the focus here is on estimating changes in current reserve volumes in response to future emissions costs, as well as demonstrating the importance of the emissions metric to calculate a illustrative emissions inventory in situations in which emissions are not constant in time. Using remaining 2P⁸ reserve and EUR data

8

[37], every⁹ gas field in the USA is mapped to the production profiles described in Section 2.1. The remaining reserves and estimated time before decommissioning are shown in Fig 6. From the emissions profiles developed in Section 3.1 this establishes the future emissions from individual fields - each of which is at a different lifecycle phase - as a function of time. The results of aggregating these future emissions using a range of CO₂ equivalencies for methane are shown in Figs. 7 and 8. Calculations using low and high estimates in Table 2 are shown also, and indicate the range in expected emissions between *individual* fields. The uncertainty in the total emissions shown here is likely to be somewhat smaller due to averaging effects (“the law of large numbers”).

The most obviously striking feature of Figs. 7 and 8 is the differences in the magnitude of GHGs depending on the choice of potential. Using dynamic potentials, central estimates of emissions in 2016 varied between 30 - 170 Mt CO₂e . A dynamic GWP with a stabilisation year of 2100 results in 79 Mt CO₂e - corresponding to $\approx 1.2\%$ of US GHG output for 2016 [65]. Static potentials (Fig 8) give an even greater range of estimates, between 26 - 174 Mt CO₂e for GTP100 and GWP20 respectively.

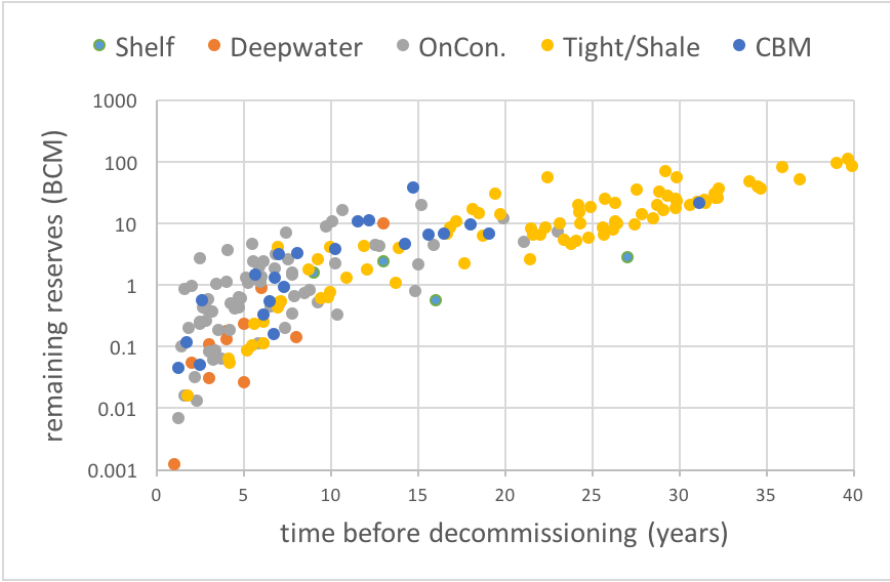


Figure 6: Remaining reserves plotted against the estimated time before decommissioning for dry natural gas fields currently producing in the USA.

All future GHG emissions scenarios show a rising trend initially after 2016, mainly due to drilling activity and several large projects ramping up production over the next 5 years. This is followed by a peak in emissions and subsequent decline. However, there are marked differences between the position

⁹Only “onstream” or “under-development” gas fields are included, and only non-associated gas fields - which produce “dry” gas or a mixture of “dry” gas and condensates - are included. This is because the emissions associated with oil extraction (and therefore the production of “non-associated” gas), are in general different.

of the emissions peak and the behaviour after 2030, depending on the methane potential. Emissions in the static cases fall off quickly, but when a dynamic potential is used the peak is shifted to later years and the subsequent reduction is more gradual. For example, the rapid growth in the GTP equivalency of methane (Fig. 1) between 20 - 40 years before the time horizon offsets the decline in aggregated methane emissions after 2025 to such an extent that the GHG trajectory in Fig. 7 (d) sustains a long plateau until around 2045 before falling off. The use of dynamic metrics is an attempt at normalising for the timing of emissions across different sources, so that - neglecting feedback effects - it is *cumulative* GHGs which determine temperature forcing at the chosen stabilisation year. However, the timing of emissions can have a significant impact on cashflows, breakeven prices, reserves and the profitability of the industry as a whole, which is in general sensitive to the timing of costs.

Fig. 9 shows cumulative GHG emissions from current US fields for all the scenarios considered. The importance of methane to overall GHGs is striking: in only 3 of the 24 scenarios does CO₂ dominate. Central estimates of cumulative GHGs using GWP potentials correspond to CO₂ combustion emissions of between 5.6 - 13.4 % of the total gas produced (meaning that this percentage of flared/own-fuel consumption would lead to a similar cumulative GHG output). The GTPs give CO₂ combustion equivalents of 2.7 - 12.9 %. Direct methane slip over the period varies between 0.40 - 0.55 % of total production.

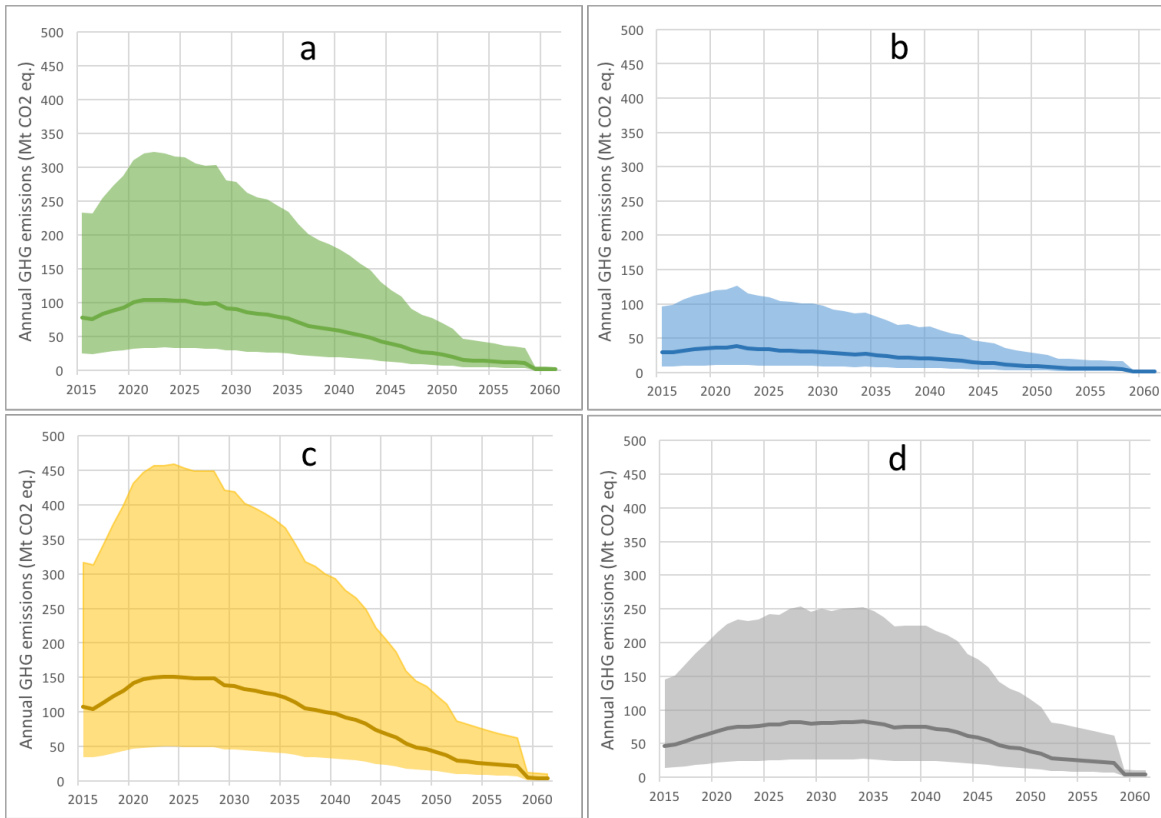


Figure 7: Total yearly GHG emissions from existing US fields using dynamic CO₂ equivalencies for methane for (a) GWP, stabilisation year 2100; (b) GTP, stabilisation year 2100; (c) GWP, stabilisation year 2065; (d) GTP, stabilisation year 2065. The shaded area spans the range between “low” and “high” estimates, and the dark line corresponds to central estimate in Table 2.

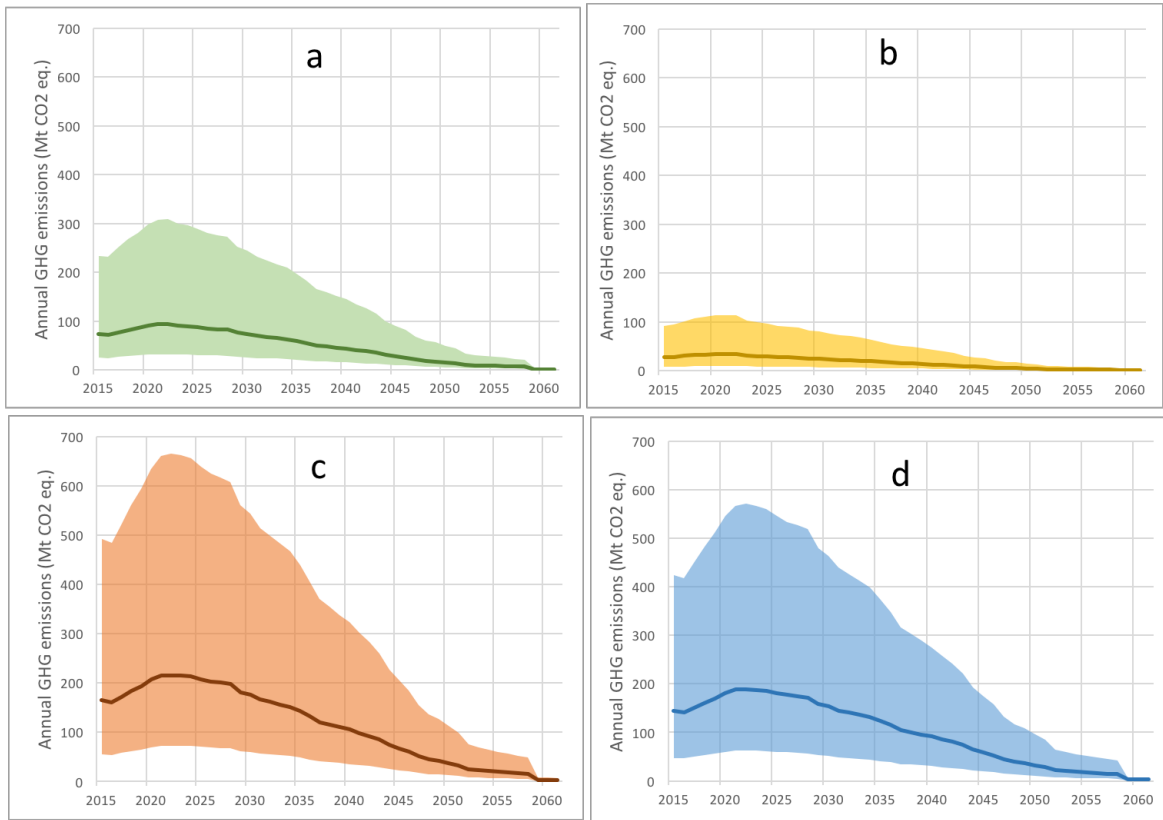


Figure 8: Total yearly GHG emissions from existing US fields using static CO₂ equivalencies for methane for (a) GWP100, (b) GTP100, (c) GWP20, (d) GTP20. The shaded area spans the range between “low” and “high” estimates, and the dark line corresponds to central estimate in Table 2.

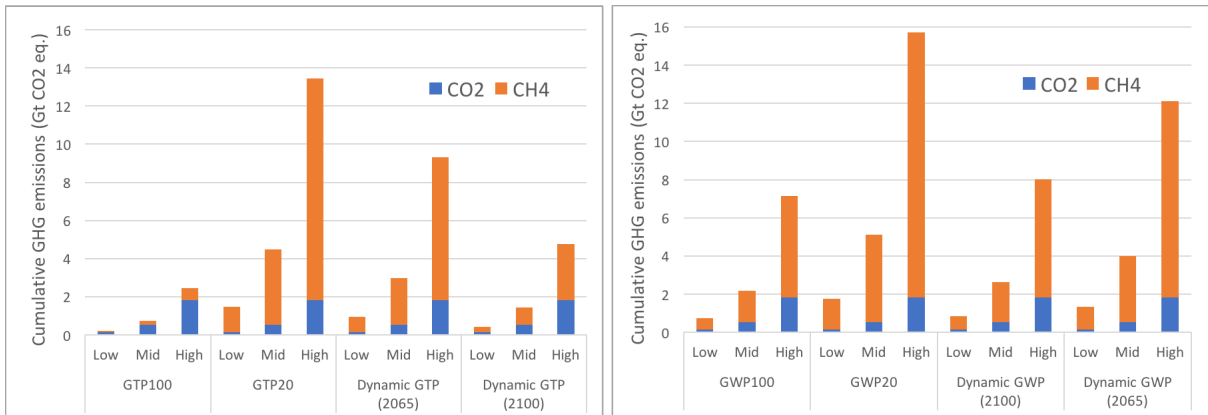


Figure 9: Cumulative future GHG emissions from existing US fields for a range of CO₂ equivalencies for methane. For dynamic potentials the stabilisation year is quoted in parentheses.

As with future emissions, the impact of a carbon price as discussed in Section 3.3 for individual fields can be investigated for the US upstream industry as a whole. By taking the suite of fields shown

in Fig. 6 and mapping them onto the expenditure profiles detailed in Section 2.1, the breakeven price of each field can be calculated as a function of both time and the forward carbon price. Assuming that producers shut-in fields when their forward NPV drops to zero, the effect of a future carbon price on cumulative GHG emissions from existing reserves is shown in Fig. 10. Four GWP methane equivalencies are considered using the central estimates in Fig. 9 (right), with emissions plotted against the average 2015 - 2050 carbon price. When the carbon price is low, cumulative GHG output is heavily dependent on the choice of methane potential, varying between 2.1 - 5.3 Gt CO₂e . Surprisingly, as the average carbon price rises above ≈ 500 USD/tonneCO₂, the cumulative emissions calculated using all four GWPs merge into one, which continues to reduce modestly as the carbon price is raised further. The 4.98% ramp-up rate corresponding to the “average conventional” carbon price scenario in Section 3.3 corresponds to an average 2015 - 2050 value of 433 USD/tonneCO₂, implying that even in this scenario the precise choice of potential for methane has a small impact on cumulative emissions.

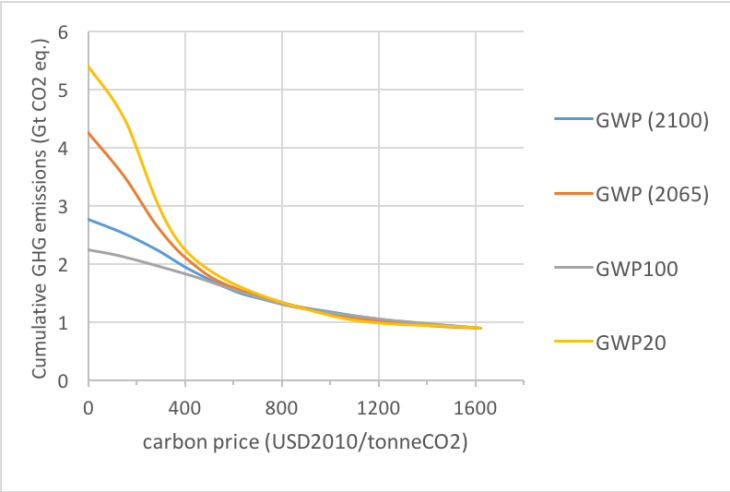


Figure 10: Cumulative future GHG emissions from existing US fields as a function of the average carbon price during the period 2015-2050. GWP (2100) and GWP (2065) use dynamic potentials for methane with stabilisation years of 2100 and 2065 respectively. GWP100 and GWP20 use static potentials for methane with a 100 year and 20 year horizon respectively.

Depending on the methane potential, the drop in cumulative GHGs by 2050 in the “average conventional” scenario is 30 - 60 % compared to the unabated scenario. This is consistent with the $\approx 50\%$ reduction in annual GHG emissions needed to constrain global warming to less than 2°C in 2100 [66]. This indicates that decarbonising the upstream component of the natural gas supply chain is achievable using carbon prices comparable to those needed for decarbonisation of the energy system as a whole.

4. Discussion and Conclusions

This study has considered the climate impacts of natural gas production and the potential economic consequences of these impacts. Using estimates of CO₂ and methane emissions for different activities in the upstream supply chain, a model of emissions profiles for conventional and unconventional fields was developed. Then, using a commercial database [63] of the EUR and remaining reserves of individual fields, this model was applied to the population of active fields in the US in order to estimate the timing and magnitude of emissions resulting from the future production of reserves in those fields. A range of carbon prices and forcing potentials for methane was used to quantify the potential economic costs of these emissions and identify the types of reserves most likely to become stranded.

As well as a very large variability in emissions levels between individual fields, it is clear that there is a strong time-dependence of emissions which is typically not considered in academic studies. The emissions profiles developed in Section 2.2 suggest that it is inappropriate to represent CO₂ output as a fixed fraction of yearly production via an “emissions intensity”, as the majority of these emissions can occur during the initial and final stages of field’s lifecycle. Under a rising carbon price, this time-dependence can have a significant bearing on breakeven prices and the volumes commercially recoverable. For methane, emissions timing can affect not only economics but also the way that climate impacts are quantified. Given their strong climate forcing but relatively short-lived nature, methane emitted further into the future - and therefore in relative temporal proximity to a set climate stabilisation year - has a disproportionately large bearing on the overall climate impact of an upstream project. For the longest-lived gas fields - which we estimate could be on-stream until around 2050 in current economic conditions - the effect is more noticeable using GTP rather than GWP CO₂ equivalency, with 40 – 50% of GHGs emitted during the last third of a typical production cycle. This favours high-value, short-cycle projects, with most large, drilling-intensive Tight/Shale projects having at least 30% of their EUR stranded for carbon prices above 400 MUSD/tonneCO₂.

This paper has estimated the variations in emissions profiles across five different field types and reports large differences in the emissions intensities associated with different stages of a field’s lifecycle. High emission scenarios show significantly higher CO₂ emissions for unconventional production compared to conventional, likely reflecting greater variations among individual plays during well completions and extraction. As around 40% of CO₂ output is directly relating to drilling activities, the timing of these emissions also depends heavily on the method of production. To describe this quantitatively, a model of drilling intensity for unconventional fields was developed based on the production profiles used in the DYNAAMO model (see Appendix A). Using this model, it has been shown that the cost of carbon embedded within the produced gas can rise at least exponentially due to increases in levelized emissions, methane climate equivalences and carbon prices. This demonstrates the high

economic risk and potential environmental burden of gas production towards 2050.

A key finding of this study is that the environmental and economic consequences of emissions are likely to rise with the age of a field, thus exposing long-lived assets to the greatest potential losses. However, we note that increases in GHG intensity towards the end of a field’s lifecycle have also been reported elsewhere in studies which either do not include methane [17] or where dynamic equivalencies for methane are not assumed [19]. In those studies the rise in GHG intensity over time has been attributed to the additional energy input required (e.g. due to enhanced recovery via fluid injections) to counter declining reservoir pressure, as well as to the greater fraction of water lifted as production decreases [67], which results in higher energy use per output of oil or gas. Because of the absence of data for this stage of recovery, the emissions profiles presented here do not account for increased energy usage due to the factors mentioned above. Given that our model applies to non-associated natural gas fields where the oil component is small, most additional late-cycle CO₂ emissions are likely to come from infill drilling, which *is* included in the drilling profile for conventional fields. However, our estimates of CO₂ emissions during the decline phase are likely to represent a lower bound on what would be found from measurements in the field.

More generally, this study has highlighted the impact of the choice of emissions metric when assessing emissions which vary as a function of time from long lived assets. The use of dynamic equivalencies for methane also changes the importance of methane as a component of total emissions. Using a dynamic rather than static GWP with a stabilisation year of 2100 increases cumulative GHGs resulting from the extraction of current US reserves by about 12%, but the methane component rises by about 18% and accounts for 80% of total emissions. Bringing forward the stabilisation year or using the dynamic GTP metric dramatically increases the importance of methane as a contributor to cumulative GHG emissions. From an climate and cost perspective, this information can help guide policymakers and E&P companies about where best to focus emissions reduction efforts.

The cumulative emissions figures in Fig. 9 correspond to average emissions intensities of 0.133 MtCO₂e/BCM (using the static GWP100). Direct comparison with the findings of other reports can be problematic, both because oil, natural gas and NGL production is often lumped together, and because emissions due to activities outside the boundary of this study are included. However, figures quoted elsewhere situate our findings among the more conservative estimates. The *Inventory of U.S. Greenhouse Gas Emissions and Sinks* reports 110.0 MtCO₂e for 2016, corresponding to an emissions intensity of 0.148 MtCO₂e/BCM for the same set of upstream activities [68]. A technical report by the *International Association of Oil and Gas Producers*, which compiles country level emissions intensities based on reported data from its member companies, estimates CO₂ and methane intensities of 201 and 2.4 kg per tonne of hydrocarbon produced respectively [69]. A breakdown by hydrocarbon type is

not provided, but we estimate corresponding¹⁰ emissions-per-volume of 0.188 MtCO₂e/BCM for 2016. This compares with with Royal Dutch Shell’s Sustainability Report for 2018, which estimates 166 kg CO₂e per tonne of hydrocarbon produced for its upstream and midstream activities [71].

The focus of this paper has been upstream emissions, not the economics of stranded assets. However, we find that a rising carbon price can make current reserves - by definition calculated with reference to the current natural gas hub price - unprofitable to extract. The “average conventional” carbon price - corresponding to an average price generated by IAMs in 2°C scenarios - strands about 21% of reserves using GWP100 and 30% using GWP2100. This can be compared to the volume of “unburnable” natural gas found by McGlade and Ekins [28], which they estimate to be about 60% of current reserves when there is a total carbon budget restricting warming to 2°C by 2100. However, McGlade and Ekins were concerned mainly with end-use (i.e. combustion) emissions, and also considered US gas reserves within the context of a global cost curve, so direct comparison is not possible.

Surprisingly, we find that for high carbon prices the choice of GHG metric has a small effect on the gross cumulative emissions resulting from the production of current reserves. For average 2015 - 2050 carbon prices above 500 USD/tonneCO₂, the carbon cost per volume of gas produced becomes larger than the NPV of that volume for the majority of asset classes. A number of projects become unprofitable to develop from the start and never end up producing, meaning that further increases in cost of carbon (which could result from either a hike in the carbon price or a higher CO₂ equivalency for methane), have a smaller impact on gross cumulative emissions. Overall, our results suggest that future cumulative GHG emissions from existing US fields have a significant short-medium term climate impact. A future CO₂ price of at least 400 USD/tCO₂ can be a successful strategy for reducing these emissions by reducing the lifetime of long-lived fields (where climate impacts are greatest) and shifting production to cleaner project types. However, such a policy is only effective if methane emissions are internalised using an appropriate CO₂ equivalency. The use of dynamic GWPs effectively accounts for the time variability in impact of future emissions and makes even modest carbon prices more effective at reducing cumulative GHG output from natural gas production.

References

- [1] G. Myhre, D. Shindell, F.-M. Bron, W. Collins, et al., *Anthropogenic and Natural Radiative Forcing.*, Cambridge University Press, Cambridge, United Kingdom and New York, NY, USA, 2013.
- [2] M. Saunio, P. Bousquet, B. Poulter, A. Peregón, et al., *The global methane budget 2000 to 2012*,

¹⁰Using a density of 0.66 kg/m³ for methane at 1.013 bar & 293K [70] and GWP100 equivalency.

- Earth Syst. Sci. Data 8 (2) (2016) 697–751. doi:10.5194/essd-8-697-2016.
URL <http://www.earth-syst-sci-data.net/8/697/2016/>
- [3] IEA, Key World Energy Statistics, Report, International Energy Agency (2016).
- [4] P. Balcombe, K. Anderson, J. Speirs, N. Brandon, A. Hawkes, The natural gas supply chain: The importance of methane and carbon dioxide emissions, ACS Sustainable Chemistry & Engineering 5 (1) (2017) 3–20. doi:10.1021/acssuschemeng.6b00144.
URL <http://dx.doi.org/10.1021/acssuschemeng.6b00144>
- [5] P. Balcombe, N. P. Brandon, A. D. Hawkes, Characterising the distribution of methane and carbon dioxide emissions from the natural gas supply chain, Journal of Cleaner Production 172 (2018) 2019–2032. doi:<https://doi.org/10.1016/j.jclepro.2017.11.223>.
URL <http://www.sciencedirect.com/science/article/pii/S0959652617328962>
- [6] EU ETS Handbook.
URL https://ec.europa.eu/clima/sites/clima/files/docs/ets_handbook_en.pdf
- [7] A. Hoover, Understanding California’s Cap-and-Trade regulations.
URL <http://www.acc.com/legalresources/quickcounsel/UCCTR.cfm>
- [8] I. B. Ocko, S. P. Hamburg, D. J. Jacob, D. W. Keith, N. O. Keohane, M. Oppenheimer, J. D. Roy-Mayhew, D. P. Schrag, S. W. Pacala, Unmask temporal trade-offs in climate policy debates, Science 356 (6337) (2017) 492–493. arXiv:<http://science.sciencemag.org/content/356/6337/492.full.pdf>, doi:10.1126/science.aaj2350.
URL <http://science.sciencemag.org/content/356/6337/492>
- [9] C. Munnings, A. Krupnick, Comparing policies to reduce methane emissions in the natural gas sector, Report, Resources for the Future (2017).
- [10] S. Hynes, K. Morrissey, C. ODonoghue, G. Clarke, A spatial micro-simulation analysis of methane emissions from Irish agriculture, Ecological Complexity 6 (2) (2009) 135–146. doi:<https://doi.org/10.1016/j.ecocom.2008.10.014>.
URL <http://www.sciencedirect.com/science/article/pii/S1476945X08000640>
- [11] S. Peter, The Effects of Pricing Canadian Livestock Emissions, Canadian Journal of Agricultural Economics/Revue canadienne d’agroeconomie 66 (2) (2018) 305–329. doi:doi:10.1111/cjag.12157.
URL <https://onlinelibrary.wiley.com/doi/abs/10.1111/cjag.12157>

- [12] M. R. Edwards, J. E. Trancik, Climate impacts of energy technologies depend on emissions timing, *Nature Clim. Change* 4 (5) (2014) 347–352. doi:10.1038/nclimate2204<http://www.nature.com/nclimate/journal/v4/n5/abs/nclimate2204.html#supplementary-information>.
URL <http://dx.doi.org/10.1038/nclimate2204>
- [13] A. Levasseur, P. Lesage, M. Margni, L. Deschnes, R. Samson, Considering Time in LCA: Dynamic LCA and its Application to Global Warming Impact Assessments, *Environmental Science & Technology* 44 (8) (2010) 3169–3174. doi:10.1021/es9030003.
URL <http://dx.doi.org/10.1021/es9030003>
- [14] M. Roy, M. R. Edwards, J. E. Trancik, Methane mitigation timelines to inform energy technology evaluation, *Environmental Research Letters* 10 (11) (2015) 114024.
URL <http://stacks.iop.org/1748-9326/10/i=11/a=114024>
- [15] M. van den Berg, A. F. Hof, J. van Vliet, D. P. van Vuuren, Impact of the choice of emission metric on greenhouse gas abatement and costs, *Environmental Research Letters* 10 (2) (2015) 024001.
URL <http://stacks.iop.org/1748-9326/10/i=2/a=024001>
- [16] S. C. Neubauer, J. P. Megonigal, Moving beyond global warming potentials to quantify the climatic role of ecosystems, *Ecosystems* 18 (6) (2015) 1000–1013. doi:10.1007/s10021-015-9879-4.
URL <https://doi.org/10.1007/s10021-015-9879-4>
- [17] E. Gavenas, K. E. Rosendahl, T. Skjerpen, CO₂-emissions from norwegian oil and gas extraction, *Energy* 90 (2015) 1956 – 1966. doi:<https://doi.org/10.1016/j.energy.2015.07.025>.
URL <http://www.sciencedirect.com/science/article/pii/S0360544215009202>
- [18] A. R. Brandt, Oil depletion and the energy efficiency of oil production: The case of California, *Sustainability* 3 (10) (2011) 1833–1854. doi:10.3390/su3101833.
URL <http://www.mdpi.com/2071-1050/3/10/1833>
- [19] M. S. Masnadi, A. R. Brandt, Climate impacts of oil extraction increase significantly with oilfield age, *Nature Climate Change* 7 (2017) 551. doi:10.1038/nclimate3347<https://www.nature.com/articles/nclimate3347#supplementary-information>.
URL <http://dx.doi.org/10.1038/nclimate3347>
- [20] H. L. Brantley, E. D. Thoma, W. C. Squier, B. B. Guven, D. Lyon, Assessment of methane emissions from oil and gas production pads using mobile measurements, *Environmental Science & Technology* 48 (24) (2014) 14508–14515. doi:10.1021/es503070q.
URL <http://dx.doi.org/10.1021/es503070q>

- [21] M. Jiang, W. M. Griffin, C. Hendrickson, P. Jaramillo, J. VanBriesen, A. Venkatesh, Life cycle greenhouse gas emissions of Marcellus shale gas, *Environmental Research Letters* 6 (3) (2011) 034014.
URL <http://stacks.iop.org/1748-9326/6/i=3/a=034014>
- [22] A. Herbst, F. A. Toro, F. Reitze, E. Jochem, Introduction to energy systems modelling, *Swiss Journal of Economics and Statistics (SJES)* 148 (II) (2012) 111–135.
URL <http://EconPapers.repec.org/RePEc:ses:arsjes:2012-ii-2>
- [23] L. M. Hall, A. R. Buckley, A review of energy systems models in the UK: Prevalent usage and categorisation, *Applied Energy* 169 (2016) 607 – 628. doi:<http://dx.doi.org/10.1016/j.apenergy.2016.02.044>.
URL <http://www.sciencedirect.com/science/article/pii/S0306261916301672>
- [24] J. Weyant, Some contributions of integrated assessment models of global climate change, *Review of Environmental Economics and Policy* 11 (1) (2017) 115–137. arXiv:[/oup/backfile/content_public/journal/reep/11/1/10.1093_reep_rew018/7/rew018.pdf](http://oup/backfile/content_public/journal/reep/11/1/10.1093_reep_rew018/7/rew018.pdf), doi: 10.1093/reep/rew018.
URL <http://dx.doi.org/10.1093/reep/rew018>
- [25] M. Roser, Our World in Data, accessed: 07-06-2018.
URL <https://ourworldindata.org/fossil-fuels>
- [26] R. Vanner, Energy use in offshore oil and gas production: trends and drivers for efficiency from 1975 to 2025, Policy Studies Institute (PSI) Working Paper, September.
- [27] R. Heede, N. Oreskes, Potential emissions of CO₂ and methane from proved reserves of fossil fuels: An alternative analysis, *Global Environmental Change* 36 (2016) 12 – 20. doi:<https://doi.org/10.1016/j.gloenvcha.2015.10.005>.
URL <http://www.sciencedirect.com/science/article/pii/S0959378015300637>
- [28] C. McGlade, P. Ekins, The Geographical Distribution of Fossil Fuels unused when limiting Global Warming to 2°C, *Nature* 517 (2015) 187–190. doi:[doi:10.1038/nature14016](https://doi.org/10.1038/nature14016).
- [29] R. Effort, L. K. Busch, Review of Natural Gas Models, Gas.
URL <https://www.eia.gov/outlooks/documentation/workshops/pdf/review%20of%20natural%20gas%20models.pdf>
- [30] A. A. Goryachev, World gas models, *Studies on Russian Economic Development* 26 (4) (2015) 327–337. doi:[10.1134/S107570071504005X](https://doi.org/10.1134/S107570071504005X).
URL <http://dx.doi.org/10.1134/S107570071504005X>

- [31] J. Tilton, B. Skinner, *The Meaning of Resources*, Resources and World Development, Wiley & Sons, New York, 1987.
- [32] H. Rogner, An Assessment of World Hydrocarbon Resources, *Annual Review of Energy and the Environment* 22 (1) (1997) 217–262. doi:10.1146/annurev.energy.22.1.217.
- [33] A. Venkatesh, P. Jaramillo, W. M. Griffin, H. S. Matthews, Uncertainty in life cycle greenhouse gas emissions from united states natural gas end-uses and its effects on policy, *Environmental Science & Technology* 45 (19) (2011) 8182–8189, pMID: 21846117. arXiv:<https://doi.org/10.1021/es200930h>, doi:10.1021/es200930h.
URL <https://doi.org/10.1021/es200930h>
- [34] T. Stephenson, J. E. Valle, X. Riera-Palou, Modeling the Relative GHG Emissions of Conventional and Shale Gas Production, *Environmental Science & Technology* 45 (24) (2011) 10757–10764, pMID: 22085088. arXiv:<https://doi.org/10.1021/es2024115>, doi:10.1021/es2024115.
URL <https://doi.org/10.1021/es2024115>
- [35] F. O. Sullivan, S. Paltsev, Shale gas production: potential versus actual greenhouse gas emissions, *Environmental Research Letters* 7 (4) (2012) 044030.
URL <http://stacks.iop.org/1748-9326/7/i=4/a=044030>
- [36] Rystad, UCube (upstream database) (2015).
URL <https://www.rystadenergy.com/Products/EnP-Solutions/UCube/Default>
- [37] Wood Mackenzie, Upstream Data Tool (2016).
URL <https://www.woodmac.com/research/products/upstream/upstream-data-tool/>
- [38] D. J. G. Crow, S. Giarola, A. D. Hawkes, A dynamic model of global natural gas supply, *Applied Energy* 218 (2018) 452 – 469. doi:<https://doi.org/10.1016/j.apenergy.2018.02.182>.
URL <http://www.sciencedirect.com/science/article/pii/S0306261918303167>
- [39] J. G. Englander, A. R. Brandt, S. Conley, D. R. Lyon, R. B. Jackson, Aerial interyear comparison and quantification of methane emissions persistence in the bakken formation of north dakota, usa, *Environmental Science & Technology* 52 (15) (2018) 8947–8953, pMID: 29989804. arXiv:<https://doi.org/10.1021/acs.est.8b01665>, doi:10.1021/acs.est.8b01665.
URL <https://doi.org/10.1021/acs.est.8b01665>
- [40] R. A. Alvarez, D. Zavala-Araiza, D. R. Lyon, D. T. Allen, Z. R. Barkley, A. R. Brandt, K. J. Davis, S. C. Herndon, D. J. Jacob, A. Karion, E. A. Kort, B. K. Lamb, T. Lauvaux, J. D. Maasakkers, A. J. Marchese, M. Omara, S. W. Pacala, J. Peischl, A. L. Robinson, P. B. Shepson, C. Sweeney,

- A. Townsend-Small, S. C. Wofsy, S. P. Hamburg, Assessment of methane emissions from the u.s. oil and gas supply chain, *Science* 361 (6398) (2018) 186–188. arXiv:<http://science.sciencemag.org/content/361/6398/186.full.pdf>, doi:10.1126/science.aar7204.
URL <http://science.sciencemag.org/content/361/6398/186>
- [41] M. Omara, N. Zimmerman, M. R. Sullivan, X. Li, A. Ellis, R. Cesa, R. Subramanian, A. A. Presto, A. L. Robinson, Methane emissions from natural gas production sites in the united states: Data synthesis and national estimate, *Environmental Science & Technology* 52 (21) (2018) 12915–12925, pMID: 30256618. arXiv:<https://doi.org/10.1021/acs.est.8b03535>, doi:10.1021/acs.est.8b03535.
URL <https://doi.org/10.1021/acs.est.8b03535>
- [42] P. Balcombe, K. Anderson, J. Speirs, N. Brandon, A. Hawkes, The natural gas supply chain: The importance of methane and carbon dioxide emissions, *ACS Sustainable Chemistry & Engineering* 5 (1) (2017) 3–20. arXiv:<http://dx.doi.org/10.1021/acssuschemeng.6b00144>, doi:10.1021/acssuschemeng.6b00144.
URL <http://dx.doi.org/10.1021/acssuschemeng.6b00144>
- [43] C. L. Weber, C. Clavin, Life cycle carbon footprint of shale gas: Review of evidence and implications, *Environmental Science & Technology* 46 (11) (2012) 5688–5695, pMID: 22545623. arXiv:<https://doi.org/10.1021/es300375n>, doi:10.1021/es300375n.
URL <https://doi.org/10.1021/es300375n>
- [44] C. Bond, et al., Life-cycle Assessment of Greenhouse Gas Emissions from Unconventional Gas in Scotland (2014).
URL <https://www.climatechange.org.uk/research/projects/life-cycle-assessment-of-ghg-emissions-from-unconventional-gas-extraction-in-scotland/>
- [45] M. Omara, M. R. Sullivan, X. Li, R. Subramanian, A. L. Robinson, A. A. Presto, Methane emissions from conventional and unconventional natural gas production sites in the Marcellus shale basin, *Environmental Science & Technology* 50 (4) (2016) 2099–2107, pMID: 26824407. arXiv:<https://doi.org/10.1021/acs.est.5b05503>, doi:10.1021/acs.est.5b05503.
URL <https://doi.org/10.1021/acs.est.5b05503>
- [46] D. T. Allen, V. M. Torres, J. Thomas, D. W. Sullivan, M. Harrison, A. Hendler, S. C. Herndon, C. E. Kolb, M. P. Fraser, A. D. Hill, B. K. Lamb, J. Miskimins, R. F. Sawyer, J. H. Seinfeld, Measurements of methane emissions at natural gas production sites in the United States, *Proceedings of the National Academy of Sciences* 110 (44) (2013) 17768–17773. arXiv:[http:](http://)

[//www.pnas.org/content/110/44/17768.full.pdf](http://www.pnas.org/content/110/44/17768.full.pdf), doi:10.1073/pnas.1304880110.

URL <http://www.pnas.org/content/110/44/17768>

- [47] D. T. Allen, D. W. Sullivan, D. Zavala-Araiza, A. P. Pacsi, M. Harrison, K. Keen, M. P. Fraser, A. Daniel Hill, B. K. Lamb, R. F. Sawyer, J. H. Seinfeld, Methane emissions from process equipment at natural gas production sites in the United States: Liquid unloadings, *Environmental Science & Technology* 49 (1) (2015) 641–648, pMID: 25488307. arXiv:<https://doi.org/10.1021/es504016r>, doi:10.1021/es504016r.
URL <https://doi.org/10.1021/es504016r>
- [48] A. Burnham, J. Han, C. E. Clark, M. Wang, J. B. Dunn, I. Palou-Rivera, Life-cycle greenhouse gas emissions of shale gas, natural gas, coal, and petroleum, *Environmental Science & Technology* 46 (2) (2012) 619–627, pMID: 22107036. arXiv:<https://doi.org/10.1021/es201942m>, doi:10.1021/es201942m.
URL <https://doi.org/10.1021/es201942m>
- [49] EPA, Greenhouse Gas Reporting Program (2016).
URL www.epa.gov/enviro/facts/ghg/customized.html
- [50] A. J. Marchese, T. L. Vaughn, D. J. Zimmerle, D. M. Martinez, L. L. Williams, A. L. Robinson, A. L. Mitchell, R. Subramanian, D. S. Tkacik, J. R. Roscioli, S. C. Herndon, Methane emissions from united states natural gas gathering and processing, *Environmental Science & Technology* 49 (17) (2015) 10718–10727, pMID: 26281719. arXiv:<https://doi.org/10.1021/acs.est.5b02275>, doi:10.1021/acs.est.5b02275.
URL <https://doi.org/10.1021/acs.est.5b02275>
- [51] A. L. Mitchell, D. S. Tkacik, J. R. Roscioli, S. C. Herndon, T. I. Yacovitch, D. M. Martinez, T. L. Vaughn, L. L. Williams, M. R. Sullivan, C. Floerchinger, M. Omara, R. Subramanian, D. Zimmerle, A. J. Marchese, A. L. Robinson, Measurements of methane emissions from natural gas gathering facilities and processing plants: Measurement results, *Environmental Science & Technology* 49 (5) (2015) 3219–3227, pMID: 25668106. arXiv:<https://doi.org/10.1021/es5052809>, doi:10.1021/es5052809.
URL <https://doi.org/10.1021/es5052809>
- [52] EDF Methane Detectors Challenge, accessed: 03-01-2019.
URL <https://www.edf.org/methane-detectors-challenge>
- [53] G. Myhre, D. Shindell, F.-M. Bron, W. Collins, J. Fuglestedt, J. Huang, D. Koch, J.-F. Lamarque, D. Lee, B. Mendoza, T. Nakajima, A. Robock, G. Stephens, T. Takemura, H. Zhang, An-

thropogenic and Natural Radiative Forcing., Cambridge University Press, Cambridge, United Kingdom and New York, NY, USA, 2013.

- [54] D. Farquharson, P. Jaramillo, G. Schivley, K. Klima, D. Carlson, C. Samaras, Beyond global warming potential: A comparative application of climate impact metrics for the life cycle assessment of coal and natural gas based electricity, *Journal of Industrial Ecology* (2016) n/a–n/doi:10.1111/jiec.12475.

URL <http://dx.doi.org/10.1111/jiec.12475>

- [55] D. S. Mallapragada, B. Mignone, A consistent conceptual framework for applying climate metrics in technology life cycle assessment, *Environmental Research Letters*.

URL <http://iopscience.iop.org/10.1088/1748-9326/aa7397>

- [56] M. R. Allen, J. S. Fuglestedt, K. P. Shine, A. Reisinger, R. T. Pierrehumbert, P. M. Forster, New use of global warming potentials to compare cumulative and short-lived climate pollutants, *Nature Clim. Change* 6 (8) (2016) 773–776. doi:10.1038/nclimate2998.

URL <http://dx.doi.org/10.1038/nclimate2998>

- [57] Drilling and well completions, in: W. C. Lyons, G. J. Plisga (Eds.), *Standard Handbook of Petroleum and Natural Gas Engineering* (Second Edition), second edition Edition, Gulf Professional Publishing, Burlington, 2004, pp. 1 – 565. doi:https://doi.org/10.1016/B978-075067785-1/50016-6.

URL <http://www.sciencedirect.com/science/article/pii/B9780750677851500166>

- [58] Oil and Gas Authority Open Data, accessed: 17-07-2018.

URL <http://data-ogauthority.opendata.arcgis.com>

- [59] Oil and Gas: Field Data. offshore Gas Fields by Well., accessed: 17-07-2018.

URL <https://www.gov.uk/guidance/oil-and-gas-uk-field-data#oil-and-gas-wells>

- [60] Berr well production, accessed: 17-07-2018.

URL https://itportal.ogauthority.co.uk/information/wells/pprs/Well_production_offshore_gas_fields/offshore_gas_fields_by_well/offshore_gas_fields_by_well.htm

- [61] Personal communications with Professor Al Fraser at Imperial College London.

- [62] Reduced emission completions for hydraulically fractured natural gas wells, accessed: 04-09-2018.

URL <https://www.epa.gov/natural-gas-star-program/reduced-emission-completions-hydraulically-fractured>

- [63] Wood Mackenzie, Global Gas Model (2014).
URL https://www.woodmac.com/content/portal/energy/highlights/wk5_Nov_14/Global%20Gas%20Model%20overview.pdf
- [64] Shale gas and coal bed methane: potential sources of sustained energy in the future, accessed: 25-07-2018.
URL [https://www.ey.com/Publication/vwLUAssets/Shale_gas_and_coal_bed_methane/\\$File/Shale_gas_and_coal_bed_methane_-_Potential_sources_of_sustained_energy_in_the_future.pdf](https://www.ey.com/Publication/vwLUAssets/Shale_gas_and_coal_bed_methane/$File/Shale_gas_and_coal_bed_methane_-_Potential_sources_of_sustained_energy_in_the_future.pdf)
- [65] Sources of greenhouse gas emissions, accessed: 13-08-2018.
URL <https://www.epa.gov/ghgemissions/sources-greenhouse-gas-emissions>
- [66] IPCC, Climate Change 2014: Synthesis Report. Contribution of Working Group I, II, and III to the Fifth Assessment Report of the Intergovernmental Panel on Climate Change, Report, IPCC, Cambridge, United Kingdom and New York, NY, USA (2014).
- [67] K. Guerra, K. Dahm, S. Dunderf, Oil and gas produced water management and beneficial use in the western United States, Tech. rep., Denver, CO (2011).
- [68] EPA, Inventory of US Greenhouse Gas Emissions and Sinks: 1990 - 2016 (2018).
URL <https://www.epa.gov/ghgemissions/inventory-us-greenhouse-gas-emissions-and-sinks>
- [69] IOGP, Environmental performance indicators 2016 data, Tech. rep. (2017).
URL <https://www.iogp.org/bookstore/product/2017e-environmental-performance-indicators-2017-data/>
- [70] Revised 1996 IPCC Guidelines for National Greenhouse Gas Inventories: Reference Manual (Volume 3), accessed: 11-10-2018.
URL <https://www.ipcc-nggip.iges.or.jp/public/gl/invs6.html>
- [71] Sustainability reporting and performance data: GHG breakdown, accessed: 11-10-2018.
URL <https://www.shell.com/sustainability/sustainability-reporting-and-performance-data/performance-data/greenhouse-gas-emissions.html#vanity-aHR0cHM6Ly93d3cuc2hlbGwuY29tL2doZw>
- [72] L. Tan, L. Zuo, B. Wang, Methods of decline curve analysis for shale gas reservoirs, *Energies* 11 (3).
- [73] K. Guo, B. Zhang, K. Aleklett, M. Hk, Production patterns of eagle ford shale gas: Decline curve analysis using 1084 wells, *Sustainability* 8 (10) (2016) 1–13.
URL <https://EconPapers.repec.org/RePEc:gam:journals:v:8:y:2016:i:10:p:973-d:79082>

- [74] K. F. Riley, M. P. Hobson, S. J. Bence, *Mathematical Methods for Physics and Engineering: A Comprehensive Guide*, 2nd Edition, Cambridge University Press, 2002. doi:10.1017/CB09781139164979.
- [75] M. J. Fetkovich, M. E. Vienot, M. D. Bradley, U. G. Kiesow, Decline curve analysis using type curves: Case histories 2 (1987) 637–656.
- [76] S. V. Fernando, H. C. Ley, Chapter 11 oil and gas reserve estimation methods, in: G. Chilingarian, S. Mazzullo, H. Rieke (Eds.), *Carbonate Reservoir Characterization: A Geologic-engineering Analysis, Part I*, Vol. 30 of *Developments in Petroleum Science*, Elsevier, 1992, pp. 505 – 542. doi:[https://doi.org/10.1016/S0376-7361\(09\)70134-7](https://doi.org/10.1016/S0376-7361(09)70134-7).
URL <http://www.sciencedirect.com/science/article/pii/S0376736109701347>
- [77] M. J. Fetkovich, E. J. Fetkovich, M. Fetkovich, Useful concepts for decline curve forecasting, reserve estimation, and analysis 11 (1996) 13–22.
- [78] D. Ilk, J. Alan Rushing, A. Duane Perego, T. Blasingame, Exponential vs. hyperbolic decline in tight gas sands: Understanding the origin and implications for reserve estimates using arps’ decline curves.
- [79] L. Ayala, Y. Peng, Unified decline type-curve analysis for natural gas wells in boundary-dominated flow, *SPE Journal* 18 (1) (2013) 97–113. doi:10.2118/161095-PA.
- [80] A. N. Duong, Rate-decline analysis for fracture-dominated shale reservoirs: Part 2 14 (2011) 377–387.
- [81] United States Energy Information Administration, *The National Energy Modeling System: an Overview* (2009).
URL [https://www.eia.gov/outlooks/aeo/nems/overview/pdf/0581\(2009\).pdf](https://www.eia.gov/outlooks/aeo/nems/overview/pdf/0581(2009).pdf)
- [82] United States Energy Information Administration, *Oil and Gas Supply Module of the National Energy Modeling System* (2018).
URL [https://www.eia.gov/outlooks/aeo/nems/documentation/ogsm/pdf/m063\(2018\).pdf](https://www.eia.gov/outlooks/aeo/nems/documentation/ogsm/pdf/m063(2018).pdf)
- [83] F. Jahn, M. Cook, M. Graham, Chapter 9 Reservoir Dynamic Behaviour, Vol. 55, Elsevier, 2008, pp. 201–227. doi:[https://doi.org/10.1016/S0376-7361\(07\)00009-X](https://doi.org/10.1016/S0376-7361(07)00009-X).
URL <http://www.sciencedirect.com/science/article/pii/S037673610700009X>
- [84] B. Söderbergh, K. Jakobsson, K. Aleklett, European energy security: An analysis of future Russian natural gas production and exports, *Energy Policy* 38 (12) (2010) 7827 – 7843, special Section: Carbon Reduction at Community Scale. doi:<http://dx.doi.org/10.1016/j.enpol.2010.08>.

042.

URL <http://www.sciencedirect.com/science/article/pii/S0301421510006579>

- [85] C. Guivarch, J. Rogelj, Carbon price variations in 2°C scenarios explored (January 2017).
URL <http://pure.iiasa.ac.at/id/eprint/14685/>
- [86] S. Budinis, S. Krevor, N. MacDowell, N. Brandon, A. Hawkes, Can technology unlock 'unburnable' carbon? (2016).
URL <http://www.sustainablegasinstitute.org/technology-unlock-unburnable-carbon/>
- [87] S. Budinis, S. Krevor, N. M. Dowell, N. Brandon, A. Hawkes, An assessment of CCS costs, barriers and potential (2018).
- [88] E. Kriegler, J. P. Weyant, G. J. Blanford, V. Krey, L. Clarke, J. Edmonds, A. Fawcett, G. Luderer, K. Riahi, R. Richels, S. K. Rose, M. Tavoni, D. P. van Vuuren, The role of technology for achieving climate policy objectives: overview of the emf 27 study on global technology and climate policy strategies, *Climatic Change* 123 (3) (2014) 353–367. doi:10.1007/s10584-013-0953-7.
URL <https://doi.org/10.1007/s10584-013-0953-7>
- [89] K. Riahi, D. P. van Vuuren, E. Kriegler, et al., The shared socioeconomic pathways and their energy, land use, and greenhouse gas emissions implications: An overview, *Global Environmental Change* 42 (2017) 153 – 168. doi:<https://doi.org/10.1016/j.gloenvcha.2016.05.009>.
URL <http://www.sciencedirect.com/science/article/pii/S0959378016300681>
- [90] IEA, World Energy Model Documentation.

5. Acknowledgements

This work is supported by NERC (NE/N018656/1) and Royal Dutch Shell plc via funding of the Sustainable Gas Institute at Imperial College London. The authors also wish to thank Prof. Al Fraser for useful discussions.

Appendices

A. Drilling and emissions profiles of unconventional fields

The drilling profile describes how the drill rate, λ , changes over the lifecycle of the field. The drill rate is a measure of drilling activity and can be taken as either the number of wells drilled per month or

else as the additional length drilled per day¹¹. Table 2 specifies total emissions from drilling activity; the purpose of the model developed below is to estimate the *timing* of these emissions.

Aggregating production from individual wells. The total production from a field results from aggregating the production of many wells drilled at earlier stages in the field lifecycle. To build a simple model of this we assume that each well produces gas initially at a rate c , but that production from individual well declines exponentially¹² at a rate β . The production, q , from a well brought on-stream at time t' is thus given for times for $t > t'$ by $q(t - t') = ce^{-\beta(t-t')}$. The total production of the field, $v(t)$, follows from integrating the product of the drilling rate with the production from each well drilled¹³:

$$v(t) = \int_0^t q(t - t')\lambda(t') dt' \quad (\text{A.1})$$

Given that v and q are known functions of time, Eq.(A.1) has a straightforward solution [74],

$$\lambda(t) = \frac{1}{c}(\dot{v} + \beta v) \quad (\text{A.2})$$

where \dot{v} denotes a derivative with respect to time. The drilling profile λ is now completely specified in terms of the production profile v (see Appendix B). Inserting Eq.(B.1) into Eq. (A.2) gives,

$$\lambda(t) = \begin{cases} 0 & -N_r \leq t < 0 \\ \frac{v_p}{N_p c}(1 + \beta t) & 0 \leq t < N_p \\ \frac{\beta v_p}{c} & N_p \leq t < N_d \\ \frac{\beta - D}{c}v_p e^{-D(t - N_d)} & N_d \leq t < N \end{cases} \quad (\text{A.3})$$

The fixed part of the CO₂ emissions profile (FCO₂ ^{n,i} in Eq.(2.5)) is constructed by combining Eq.(A.3) with the data in Table 2 to give,

$$\text{FCO}_2^{n,i} = \begin{cases} \frac{1}{N_r} \cdot R_{0,i} \cdot \text{CO}_{2,\text{prep}} & -N_r \leq n < 0 \\ \bar{\lambda}(n) \cdot R_{0,i} \cdot \text{CO}_{2,\text{drill}} & 0 \leq n < N \end{cases} \quad (\text{A.4})$$

where CO_{2,prep} is the CO₂ intensity of site preparations and CO_{2,drill} is the CO₂ intensity of sub-stages associated with drilling, including well completions and hydraulic fracturing. In Eq.(A.4), $R_{0,i} \cdot \text{CO}_{2,\text{prep}}$

¹¹A continuous time formulation is adopted for tractability; differences from daily or monthly drill rates will be small for large fields in which the smallest time scale in the production profile is typically of the order of several years.

¹²Exponential decline is likely to be a simplification of real-world behaviour, especially towards the start of production. Its merit is that (retarded) drilling intensity can be related simply to production using an *effective* decline rate, and, when averaged over an ensemble of different wells, differences compared to other forms of decline curve are likely to be negligible (see [72]).

¹³This model does not account for the shutting-in of wells for which production rates are unprofitably low. This is a reasonable assumption given that (a) shut in rates have been approximated as $\approx 1.1\%$ of initial monthly production [73] and (b) that it is the *intensity* of drilling that matters for this study.

are the total CO₂ emissions from site preparations, spread over the N_r years of the pre-production phase, and $R_{0,i} \cdot \text{CO}_{2,\text{drill}}$ is the total contribution from drilling activities which is weighted by the drilling intensity $\bar{\lambda}(n) = \lambda(n) / \sum_n \lambda(n)$ over the production phase of the field. Note that $\bar{\lambda}$ (unlike λ) depends only on β and D , which avoids the need to specify the initial well production rate, c .

Estimating the well decline rate β . The fall-off in production from an individual well is a much studied area of research [75] [76] [77]. It is often modelled as going through two stages: an initial “boundary-dominated” stage in which the decline rate (i.e. “change in production” \div “production”) reduces linearly with time, followed by a “fracture-dominated” regime in which it is approximately constant [78] [79] [80] [72]. During the first stage, production, q , follows a hyperbolic curve as a function of time t , $q = q_0(1 + Dbt)^{-1/b}$, where the decline parameter D and the loss ratio b depend on the individual well characteristics and can be found from fitting to time series production data. The initial production rate q_0 is normally reported on a well-by-well basis. During the latter stage, after decline has fallen to a specified rate D_1 , production is assumed to fall-off exponentially as $q \sim e^{-D_1 t}$.

The Oil and Gas Module of the US *Energy Information Agency* NEMS model [81] [82] uses this two-stage approach, and reports b , D and q_0 values for 142 select shale gas wells taken from major US plays including Marcellus, Eagle Ford and Barnett. The NEMS analysis takes the crossover decline rate separating the two stages of production as 10% ($D_1 = 0.1$). Using these reported values of b and D it is straightforward to derive an estimate for β by equating production from a single well over the first 12 months of production using mixed (hyperbolic and exponential) and pure exponential decline curves:

$$\int_0^{12} e^{-\beta t} dt = \int_0^{t_c} (1 + bDt)^{-1/b} dt + \int_{t_c}^{12} e^{-0.1t} dt \quad (\text{A.5})$$

Here, $t_c = 0.9^b / (1 - 0.9^b) - 1/bD$ is the crossover time separating hyperbolic and exponential decline (the median value of t_c was 6.28 months and only 3 of the wells in the sample of 142 had crossover times longer than 12 months). From this analysis, the mean value of β is 0.135 with standard error 0.005. This monthly decline rate of 13.5% is consistent with first year annual decline rates of $\approx 80\%$ that have been quoted elsewhere [73].

B. The DYNAAMO model

DYNAAMO (see [38] for a full details) uses expenditure and production data from thousands of fields to build a bottom-up, field-level model of non-associated natural gas supply. The two key ingredients are the *production profile*, which describes how production from a typical field of a particular size is expected to change over time, and the *expenditure profile*, which describes yearly expected capex, opex, and fiscal (“government take”) expenditure. An illustration of these lifecycle profiles is shown in Fig. B.11.

Production profile. A reservoir follows a standard preproduction, ramp-up, plateau and decline phase [83], with the decline rate and abandonment time set endogenously using a reference forward price scenario, such that the anticipated total production equals the initial EUR. Production v is a piecewise continuous function of time t given by,

$$v(t) = \begin{cases} 0 & -N_r \leq t < 0 \\ \frac{v_p}{N_p}t & 0 \leq t < N_p \\ v_p & N_p \leq t < N_d \\ v_p e^{-D(t-N_d)} & N_d \leq t < N \end{cases} \quad (\text{B.1})$$

After discovery and appraisal of the field there is a preproduction phase lasting N_r months before a ramp-up phase lasting N_p months, during which production increases linearly, reaching a peak in month N_p . The field then produces gas “on plateau” at a constant rate v_p for a further $N_d - N_p$ months, after which production declines exponentially with decline rate D until the field is abandoned in period N . Preproduction times vary by field environment and field size, but are normally between 18 – 48 months. The ramp-up phase lasts a similar length, depending mainly on the size of the field and the decline rate of individual wells. The length of the plateau phase of production depends on the EUR. Large fields tend to produce a smaller fraction of their EUR per month on plateau than small fields, reflecting a trade-off between variable opex and the discounting of future cashflows. The result is that large fields normally produce over a longer period than small fields, although the field environment also matters, largely due to the costliness offshore operations. Based on analysis of historic production data, DYNAAMO uses a relationship of the form $v_p \sim \text{EUR}^y$ to model the plateau rate, with $y = 0.75$ or $y = 0.85$ for onshore and offshore fields respectively (this is consistent with other approaches [84]). Drilling of individual wells may continue at a lower intensity after the plateau phase to achieve a managed decline in aggregate production of the field of between 3 – 15% per year. Decommissioning occurs at the field’s “economic limit”, when the remaining NPV (which includes abandonment costs) falls to zero due to the decline in production.

Expenditure profile. Fig. B.11 shows an example of operational and capital expenditure¹⁴ (opex and capex) over the lifecycle of a small deepwater field. There will be some economic (and emissions) activity prior to the start of the pre-production phase due to the drilling of exploratory wells and seismic appraisal. However, this phase of operations is not modelled explicitly¹⁵ as it is widely variable

¹⁴Capex includes costs related to drilling, building facilities/infrastructure and exploration for new resources (“expex”). Opex includes costs directly related to running operations, such as administrative and insurance costs, equipment hire & salaries, and (often significant) abandonment costs associated with field decommissioning.

¹⁵Exploratory capex is included in annual capex, spread over the project lifecycle.

by project and has little impact on the main focus of this study. Similarly, abandonment costs are in reality spread over several years after production has ended, but for modelling simplicity this is treated as a discounted one-off payment in the final year of production. Opex and capex profiles vary considerably by field environment, reflecting both the relative importance of facilities and infrastructure costs in overall project financing, as well as the timing and intensity of drilling. Offshore fields are subject to very high capital costs, whereas for onshore unconventional fields drilling/fracking capex is spread over the whole production phase. The percentage ratio of project opex to project capex is also highly sensitive to field environment (ranging from 30% for deepwater fields to 160% for onshore conventional fields), as are decommissioning costs (which represent 16% and 5% of project capex for deepwater and onshore conventional fields respectively [37]).

Field sizes. The production and expenditure profiles of gas fields (and therefore all consequent model outputs) depend on the initial 2P EUR (denoted by R_0). This varies enormously by individual field. However, data from several thousand historic and currently-producing fields indicate that EURs are log-normally distributed, with a mean and variance characteristic of the particular field environment (see Fig. B.12). To model this diversity of field sizes - which can impact the economics of production via economies of scale¹⁶ - DYNAAMO samples the field size distributions to construct an *asset class*: a field of a specified field environment and characteristic size. Where appropriate, results for different field environments quoted in this study are volume-weighted averages over asset classes.

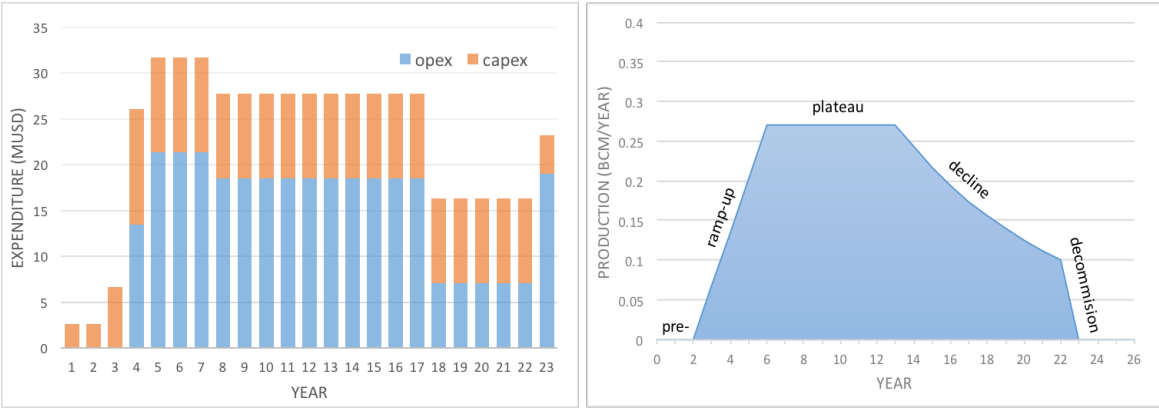


Figure B.11: The expenditure profile (left) and production profile (right) of a representative 4.5 BCM *Coal Bed Methane* field. On plateau the field produces about 6% of its Estimated Ultimate Recovery (EUR) per year, before production enters a managed exponential decline of 11% per year. The field is decommissioned when its remaining NPV drops to zero due to the decline in production. Capex is dominated by well-capex, spread over the production cycle, and the opex/capex ratio is 1.57. Note that abandonment opex in year 23 is paid over a decommissioning period equal to the lead time in DYNAAMO.

¹⁶DYNAAMO uses a relation of the form ‘project capex \sim EUR^{2/3}’.

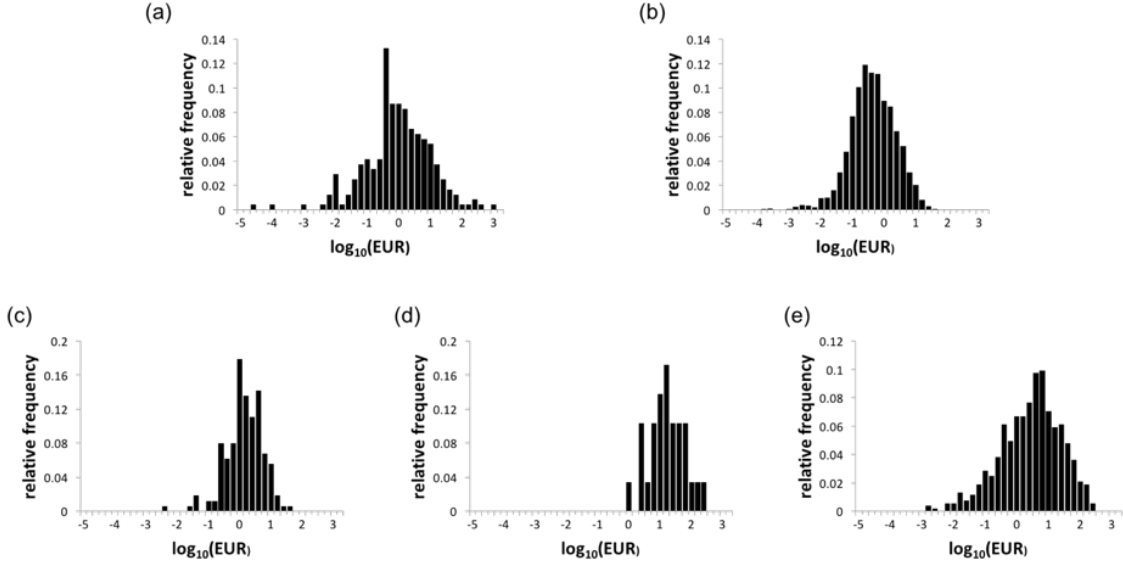


Figure B.12: Field size distributions showing the relative frequency of vs the log of the initial 2P EUR (in BCM) for (a) Onshore Conventional, (b) Shelf, (c) Deep Offshore, (d) CBM, (e) Tight/Shale. The bin width is 0.2.

NPV & the breakeven price. The lowest price at which a rational producer will still offer gas to the market is known as the *breakeven price*. This is typically highest at the start of a project cycle, and drops rapidly once major capital costs have been paid off. DYNAAMO calculates breakevens from current and future expected cashflows. The cashflow in year n of a project is given by,

$$\text{cashflow}_{t,n,i} = (p_t - \text{cpr}_t \cdot \text{VE}_{t,n,i}) v_{n,i} - (\text{capex}_{n,i} + \text{opex}_{n,i} + \text{cpr}_t \cdot \text{FE}_{n,i}) \quad (\text{B.2})$$

where $v_{n,i}$ is production, p_t is the gas price, cpr_t is the carbon price and $\text{capex}_{n,i} + \text{opex}_{n,i}$ is annual expenditure (broken down into capex and opex). The subscripts i and t refer to the asset class and model year respectively. Emissions costs are assumed to be paid concurrently with emissions and comprise a variable ($\text{VE}_{t,n,i}$) and fixed ($\text{FE}_{n,i}$) component (explained in Section 2.2). The sum of discounted future cashflows gives the net present value (NPV) of a field, and the gas price for which the NPV vanishes is taken as the breakeven of that field in a given year. In line with other academic reports and industrial practice, this study uses a fixed 10% discount rate throughout.

C. Carbon price trajectories

Although direct taxation on carbon emissions is currently uncommon, carbon prices are widespread in studies of decarbonisation using energy- and integrated assessment models (IAMs). In low emissions scenarios, models typically assume or generate a shadow price for carbon which can represent the cost of abatement or policy instruments, including carbon pricing. Due to differences in both modelling

approaches and assumptions regarding the availability and cost of low-carbon technologies, there is often a large variation in the future carbon prices generated. One review of outputs from IAM studies of 2°C scenarios reports carbon prices between 15 - 360 USD2005/tonneCO₂ in 2030 and 45 - 1000 USD2005/tonneCO₂ in 2050 [85]. For the present study, a sensitivity analysis is performed over a range of plausible carbon prices based on the findings of a recent assessment of Carbon Capture and Storage (CCS) [86] [87]. That study considered 18 IAMs which went into a model inter-comparison undertaken by the Energy Modelling Forum (EMF27) at Stanford University, based on scenarios which limited CO₂e to less than 450 ppm in 2100 [88]. Three different technology scenarios were selected, and the average carbon price calculated for each scenario. The full technology scenario (“Fulltech”) has a full portfolio of technologies which may scaled up in the future in order to meet the climate targets; the average conventional (“Conv”) scenario limits the growth of renewables but allows CCS deployment; the scenario without CCS (“noCCS”) is the same as the “Fulltech” scenario but CCS never becomes available [89] [88]. In order to use the carbon price as a continuous input variable, a function of the form $cpr_t = \alpha_1 + \exp(\alpha_2 + \gamma t)$ was fitted to the “Conv” scenario over the period 2010 - 2070, for which $\alpha_1 = -152.1$, $\alpha_2 = 5.129$ and $\gamma = 0.04978$ (corresponding to a ramp up rate of $\approx 5.0\%$). The sensitivity analysis then follows by holding α_1 and α_2 fixed while varying γ continuously.

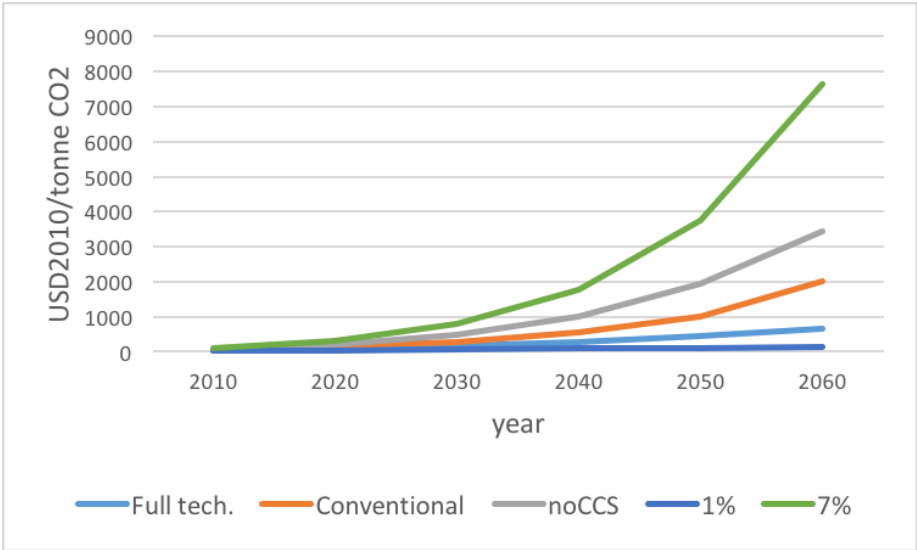


Figure C.1: A range of carbon price trajectories to 2100 consistent with 2°C warming. The “conventional” scenario has a ramp rate of $\approx 5\%$. Trajectories corresponding to 1% and 7% ramp up rates are shown for reference.

This method gives ramp up rates of 3.1% and 5.8% for the “Fulltech” and “noCCS” scenarios respectively; for generality this study will consider an envelope of ramp up rates varying between 0%–7%. Fig. C.1 shows representative carbon price trajectories as well as the three reference scenarios discussed above. Due to the exponential growth, carbon prices after 2050 can grow very high; for

context, the cost of carbon assumed by the IEA [90] for the 450 Scenario (140 USD/tonneCO₂ in most OECD countries in 2040) corresponds to a ramp up rate of 1.6 %. To better represent the exponential growth of the carbon price, the average carbon price in the period 2010 - 2050 is quoted in preference to the ramp up rate in this study.